pharmacological approach, Cyclosporine A (CsA), which binds to Cyp D to inhibit MPT (Halestrap and Davidson, 1990), and its analogs (*N*-methyl-val[4]-cyclosprin and FR901459) prevent neuronal degeneration in ischemia models (Matsumoto et al., 1999; Muramatsu et al., 2007). These results suggest that Cyp D and MPT is therapeutic target for these degenerative disorders.

Although, as aforementioned, a pathological role of Cyp D and MPT has been uncovered, their physiological role remains elusive. Mitochondria assist in maintaining Ca^{2+} homeostasis by sequestering and releasing Ca^{2+} (Bernardi, 1999; Nicholls and Budd, 2000). Synaptic mitochondria are synthesized in the cell body of neurons and transported to axons and dendrites (Morris and Hollenbeck, 1993; Kang et al., 2008). Mitochondria are present at high concentrations in presynaptic terminals (Shepherd and Harris, 1998; Rowland et al., 2000; Brown, 2006). Neurotransmitter release is driven by an elevation of the Ca^{2+} concentration within the presynaptic terminal (Dodge and Rahamimoff, 1967; Long et al., 2008). Thus, some researchers have reported that mitochondria play a pivotal role in the release of neurotransmitters and short-term plasticity (Tang and Zucker, 1997; Billups and Forsythe, 2002; Lee et al., 2007; Kang et al., 2008). Under physiological conditions, Cyp D-dependent MPT has been suggested to be involved in Ca^{2+} buffering and thus to play an important role in learning and memory, and synaptic plasticity (Weeber et al., 2002; Levy et al., 2003). CsA impairs long-term potentiation (LTP) and prepulse facilitation (Levy et al., 2003), and mice lacking VDAC isoforms show deficits in spatial and associative learning and synaptic plasticity (Weeber et al., 2002). Conversely, mice lacking Cyp D shows enhanced response in avoidance tests (Luvisetto et al., 2008) and normal synaptic plasticity and spatial memory in radial water maze test (Du et al., 2008). Further behavioral experiments are needed for exploring the roles of CypD in learning and memory.

In the present study, we investigated the performance of several learning and memory tasks in mice lacking Cyp D and mice infused with CsA into the hippocampus, and found cognitive dysfunction.

MATERIALS AND METHODS

Mice

Male C57BL/6J mice (7 weeks old) were obtained from Japan SLC (Shizuoka, Japan). Mice lacking Cyp D were described by Nakagawa et al. (2005). The homozygous mutant male mice (−/−; 3 months of age) and the littermate wild-type male mice (+/+; 3 months of age) were obtained by crossing F10 heterozygous Cyp D mutant mice (±) having a 99.99% pure C57BL/6J genetic background. The genotypes of mice were determined by PCR (Fig. 1A). The wild-type allele (553 bp) was detected using 5′-GCAGATCAAGCTCCC GACTG-3′ as a forward primer and 5′-ACTTGGGAAGCC GAGGTG-3′ as a reverse primer. To detect the mutant allele (206 bp), a neomycin-specific reverse primer (5′-GCAGCG CATCGCCTTCTATC-3′) was used in combination with the wild-type forward primer as described by Nakagawa et al. (2005). The animals were housed in plastic cages and kept in a regulated environment (24 ± 1°C, 50 ± 5% humidity), with a 12-h light/dark cycle (lights on at 9:00 AM). Food and tap water were available ad libitum. All experiments were performed in accordance with the Guidelines for Animal Experiments of Meijo University. The procedures involving animals and their care were conducted in conformity with the international guidelines, Principles of Laboratory Animal Care (National Institutes of Health publication 85–23, revised 1985).

Surgery

Under anesthesia (pentobarbital 40 mg/kg, i.p.), C57BL/6J mice were placed in a stereotaxic apparatus and bilaterally implanted with a guide cannula (12 mm, 0.4 mm in inner diameter, 0.5 mm in outer diameter; Eicom) in the hippocampus (−2.2 mm anteroposterior, ±2.0 mm mediolateral from the bregma, −1.5 mm dorsoventral from the skull) according to the atlas of Paxinos and Franklin (2004). A dummy cannula (0.3 mm in diameter; Eicom) was left in place throughout the experiment. Five days after the operation, mice were subjected to the novel object recognition test or conditioned fear learning test.

Drug Treatment

CsA obtained from Novartis Pharmaceuticals (Basel, Switzerland) was dissolved in ethyl alcohol/polyethoxylated castor oil (35/65). For microinjection into the hippocampus, a 28-gauge injection cannula (Eicom) cut to extend 1.0 mm beyond the guide cannula was inserted through the guide cannula. Among the known targets of CsA, Cyp D has one of the lowest Ki values in vitro (Galat, 1993). However, one specific concern with the use of CsA to block Cyp D is the possibility of inhibition of the protein phosphatase, calcineurin. Levy et al. (2003) have reported that high doses (250 μM) of CsA inhibit calcineurin in the hippocampal slice by measuring the phosphorylation state of a calcineurin substrate, synapsin I. Considering these reports and diffusion of CsA in hippocampus, CsA was diluted with artificial cerebrospinal fluid (CSF: 147 mM NaCl, 4 mM KCl, and 2.3 mM $CaCl_2$) at a concentration of 100 μM and injected bilaterally (100 pmol/1.0 μl/side) over a 5-min period 10 min before the training session in the novel object recognition test or the conditioning session in the conditioned fear learning test.

Behavioral Analysis

A battery of behavioral experiments was carried out according to previous reports (Mouri et al., 2007a). The behavioral tests were carried out sequentially with the Y-maze test, Novel-

Hippocampus

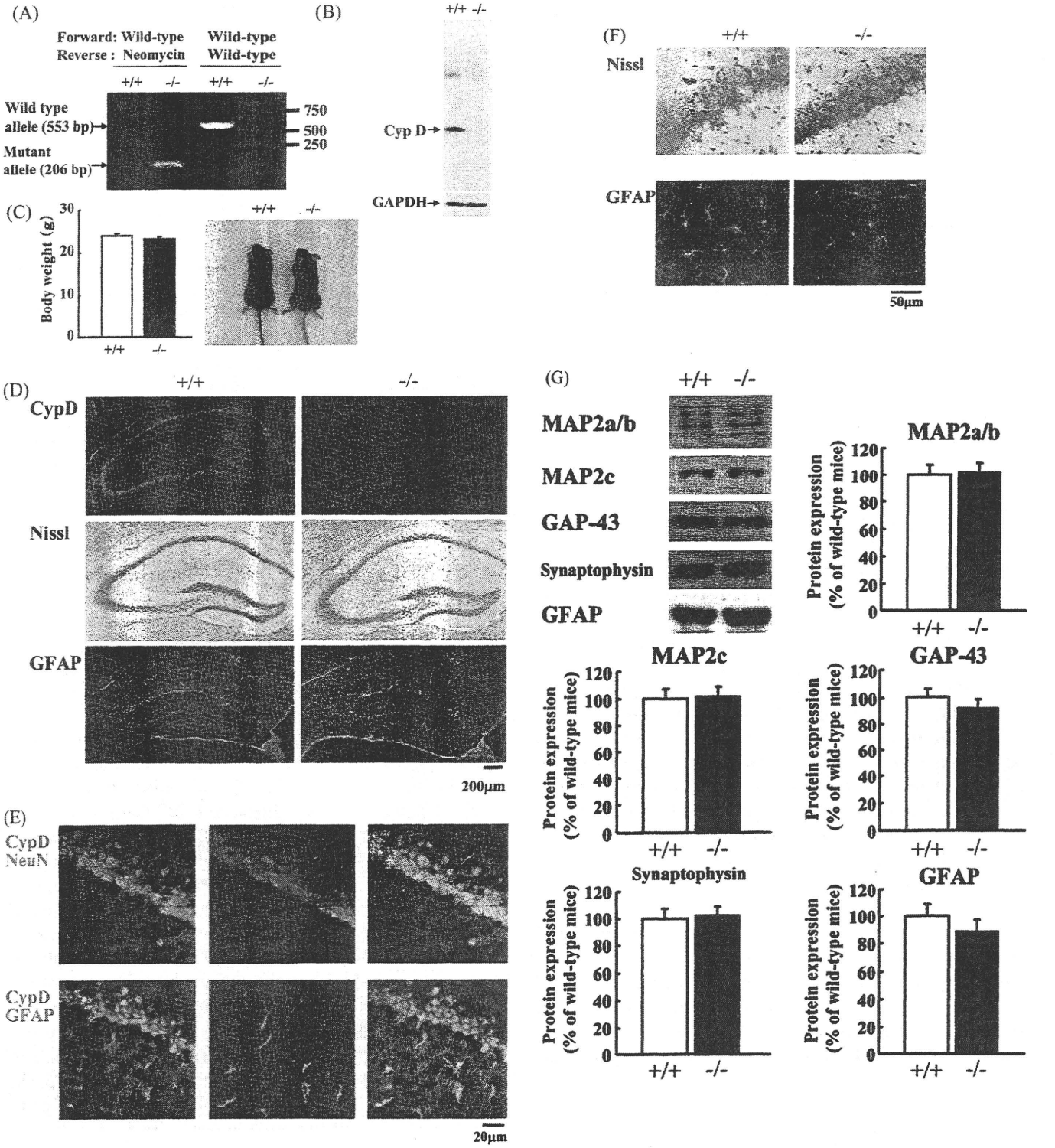

FIGURE 1. Histological characterization of Cyclophilin D and Cyclophilin D-deficient mice. (A) Determination of genotype: Genotyping was performed by PCR and gel electrophoresis. The wild-type allele (553 bp) and mutant allele (206 bp) were identified by PCR using wild-type forward and reverse primers and the wild-type forward primer and neomycin-specific reverse primer, respectively. (B) Protein expression of Cyp D in Cyp $D^{-/-}$ mice: Protein extracts from the whole brain of Cyp $D^{-/-}$ and wild type mice were examined by Western blotting. (C) Representative examples of wild-type and Cyp $D^{-/-}$ mice at 3 month: Body weights of wild-type and Cyp $D^{-/-}$ mice were 23.9 ± 0.44 and 23.0 ± 0.65 g, respectively. (D) Cyp D-, GFAP-immunostaining, and Nissl staining in the Cyp $D^{-/-}$ and wild-type mice: Slices of hippocampus obtained from Cyp $D^{-/-}$ mice showed no immunoreactivity to anti-Cyp D antibody and no abnormal structure or glial distribution. (E) Localization of Cyp D in the hippocampus: Confocal immunofluorescent images obtained from coronal sections of wild-type mice. Cyp D immunoreactivity was evident in neuronal cell layers in CA1 and localized to cells positive for NeuN, a marker of neuronal cells. Enhanced sensitivity revealed Cyp D immunoreactivity in cells positive for GFAP, a marker of astrocytes. (F) A higher magnitude image of the hippocampal CA1 region. There was no morphological change to neuronal cells and astrocytes in Cyp $D^{-/-}$ mice. (G) Western blotting of homogenates from the hippocampus for proteins described. No difference was observed between the two genotypes (wild-type mice, $n = 10$; Cyp $D^{-/-}$ mice, $n = 10$; Student t-test). +/+, wild-type mice; −/−, Cyp $D^{-/-}$ mice.

object recognition test, Morris water maze test, and Cued and contextual fear conditioning tests.

Spontaneous Alternation in a Y-Maze Test

The maze was made of black-painted wood; each arm was 40 cm long, 12 cm high, 3 cm wide at the bottom, and 10 cm wide at the top. The arms converged at an equilateral triangular central area that was 4 cm at its longest axis. Each mouse was placed at the center of the apparatus and allowed to move freely through the maze during an 8-min session. The series of arm entries was recorded visually. Alternation was defined as successive entry into the three arms, on overlapping triplet sets. The alternation behavior (%) was calculated as the ratio of actual alternations to possible alternations (defined as the number of arm entries minus two), multiplied by 100.

Novel-Object Recognition Test

The test procedure consisted of three sessions: habituation, training, and retention. Each mouse was individually habituated to the Plexiglas box (30 × 30 × 35 cm^3 high), with 10 min of exploration in the absence of objects for 3 days (habituation session). During the training session, two objects were placed in the back corner of the box. The objects were a golf ball, wooden cylinders, and square pyramids, which were different in shape and color but similar in size. A mouse was then placed midway at the front of the box and the total time spent exploring the two objects was recorded for 10 min. An animal was considered to be exploring the object when its head was facing the object or it was touching or sniffing the object. During the retention session, the animals were placed back into the same box 24 h after the training session, in which one of the familiar objects used during training was replaced with a novel object. The animals were then allowed to explore freely for 10 min and the time spent exploring each object was recorded. Throughout the experiments, the objects were used in a counterbalanced manner in terms of their physical complexity and emotional neutrality. A preference index, a ratio of the amount of time spent exploring any one of the two objects (training session) or the novel object (retention session) over the total time spent exploring both objects was used to measure cognitive function.

Morris Water Maze Test

The Morris water maze test was conducted in a circular pool 1.2 m in diameter and filled with water at a temperature of 22 ± 1°C. A hidden platform (7 cm in diameter) was used. The mice were given two trials (one block), 60 s each trial, for 10 consecutive days, during which the platform was left in the same position. The time taken to reach to the escape platform (escape latency) was determined in each trial by using the Etho Vision system (Brainscience Idea, Osaka, Japan). Three hours after the last training trial, the mice were given a probe test without the platform and were allowed 60 s to search the pool.

Cued and Contextual Fear Conditioning Tests

For measuring basal levels of freezing response (preconditioning phase), mice were individually placed in a neutral cage (17 × 27 × 12.5 cm^3 high) for 1 min and then in the conditioning cage (25 × 31 × 11 cm^3 high) for 2 min. For training (conditioning phase), mice were placed in the conditioning cage, and then a 15-s tone (80 dB) was delivered as a conditioned stimulus. During the last 5 s of the tone stimulus, a foot shock of 0.6 mA was delivered as an unconditioned stimulus through a shock generator (Brainscience Idea). This procedure was repeated four times with 15-s intervals. Cued and contextual tests were carried out 1 day after fear conditioning. For the cued test, the freezing response was measured in the neutral cage for 1 min in the presence of a continuous-tone stimulus identical to the conditioned stimulus. For the contextual test, mice were placed in the conditioning cage, and the freezing response was measured for 2 min in the absence of the conditioned stimulus.

Western Blot Analysis

Western blotting was performed as previously described (Mouri et al., 2007b). The mice were sacrificed by decapitation, and the brain was immediately removed. The hippocampus was rapidly dissected out on an ice-cold plate, frozen, and stored at −80°C until used. To prepare tissue extracts, the dissected brain tissue was homogenized by sonication in an ice-cold lysis buffer [20 mM Tris–HCl (pH 7.4), 150 mM NaCl, 50 mM NaF, 2 mM EDTA, 0.1% sodium dodecyl sulfate (SDS), 1% sodium deoxycholate, 1% NP-40, 1 mM sodium orthovanadate, 20 μg/ml pepstatin, 20 μg/ml aprotinin, and 20 μg/ml leupeptin]. The homogenate was centrifuged at 13,000*g* for 20 min and the supernatant was used. The protein concentration was determined using a DC Protein Assay Kit (Bio-Rad, Richmond, CA). Samples (10–100 μg of protein) were boiled in sample buffer (125 mM Tris–HCl, pH 6.8, 10% 2-mercaptoethanol, 4% sodium diphosphate decahydrate, 10% sucrose, and 0.004% bromophenol blue), separated on a polyacrylamide gel, and subsequently transferred to polyvinylidene difluoride (PVDF) membranes (Millipore, Billerica, MA). The membranes were blocked with a Detector Block Kit (Kirkegaard and Perry Laboratories, Gaithersburg, MD) and probed with a primary antibody. Membranes were washed with the washing buffer [50 mM Tris–HCl (pH 7.4), 0.05% Tween 20, and 150 mM NaCl] and subsequently incubated with a horseradish peroxidase-conjugated secondary antibody. The immune complexes were detected based on chemiluminescence (ECL kit, Amersham Biosciences, Piscataway, NJ) and exposed to X-ray film (Hyperfilm, Amersham Biosciences). The band intensities on the film were analyzed by densitometry using the ATTO Densitograph Software Library Lane Analyzer (ATTO, Tokyo, Japan). To confirm equal loading of each protein, membranes were stripped with stripping buffer [100 mM 2-mercaptoehanol, 2% SDS, and 62.5 mM Tris–HCl (pH 6.7)] at 50°C

for 30 min, and GAPDH protein expression was detected as described above.

The primary antibodies were a rabbit anti-CyP D [1:1,000; synthesized by the authors using a peptide (aa 43–57) of Cyp D], a mouse anti-MAP2 (1:1,000; Chemicon, Temecula, CA), a rabbit antigrowth associated protein (GAP)-43 (1:1,000; Chemicon), a mouse antiglial fibrillary acidic protein (GFAP) (1:1,000; Chemicon), a rabbit antisynaptophysin (1:1,000; Dako, Glostrup, Denmark), a guinea pig antiglutamate transporter GLAST and a guinea pig anti-GLT-1 (1:1,000; Chemicon), a mouse antiglutaminase (GLS) (1:500; Abnova, Taipei, Taiwan), a mouse anti-NR1 CT (1:1,000; Upstate Biotechnology, Lake Placid, NY), a mouse anti-NMDAR2A and a mouse anti-NMDAR2B (1:1,000; BD Pharmingen, San Diego, CA), a rat anti-ChAT (Calbiochem, San Diego, CA), and a goat anti-ACHE (E-19) (1:500; Santa Cruz Biotechnology, Santa Cruz, CA). The secondary antibodies, used at a dilution of 1:2,000, were horseradish peroxidase-linked antimouse, antirabbit, antirat, or antiguinea pig IgG (Kirkegaard and Perry Laboratories).

Preparation of Brain Slice and Staining

Histological procedures were performed as previously described with a minor modification (Murai et al., 2007). Mice were anesthetized with chloral hydrate (150 mg/kg i.p.) and perfused transcardially with ice-cold phosphate-buffered saline (PBS), followed by 4% paraformaldehyde in PBS. The brains were removed, postfixed in the same fixative for 2 h, and then soaked in 20% (w/v) sucrose in PBS. Coronal sections 15 μm thick were cut with a Cryostar HM560 cryostat (Microm International, GmbH, Walldorf, Germany). For immunohistochemistry, the primary antibodies that were applied in the brain slices included a rabbit anti-Cyp D (1:500; synthesized by the authors), a mouse antineuron-specific nuclear antigen (NeuN) (1:500; Chemicon) and mouse anti-GFAP (1:500; Chemicon) antibody. Fluorescently conjugated secondary antibodies (Alexa 488, 546, Invitrogen, Carlsbad, CA) were used for detecting chromagen. For Nissl staining, sections were cut at 40-μm intervals and staining was done according to standard procedures (Murai et al., 2007). Images were acquired with a confocal microscope (LSM510; Carl Zeiss, Jena, Germany) and a light microscope (Axiocam HRc; Carl Zeiss).

In Vivo Microdialysis

In vivo microdialysis was performed as previously described (Mouri et al., 2007b; Murai et al., 2007). Mice were anesthetized with sodium pentobarbital (40 mg/kg i.p.) before the stereotaxic implantation of a guide cannula (AG-6, Eicom, Kyoto, Japan) into the ventral hippocampus (−2.8 mm anteroposterior, ±3.0 mm mediolateral from the bregma, −2.0 mm dorsoventral from the skull). One day after the operation, a dialysis probe (AI-4–2; 2-mm membrane length, Eicom) was inserted through the guide cannula and perfused with CSF (147 mM NaCl, 4 mM KCl, and 2.3 mM $CaCl_2$) at a flow rate of 1 μl/min. The dialysate was colleted every 20 min. Dialysates were assayed by HPLC with electrochemical detection (HTEC-500, Eicom) under the following conditions. Three samples were taken to establish baseline levels of extracellular neurotransmitter. For depolarization stimulation, 50 mM KCl-containing Ringer solution was delivered through the dialysis probe for 20 min to induce the K^+-evoked release of glutamate and acetylcholine (ACh). Then dialysate was collected for 20 min with ringer solution.

Statistic Analysis

All results were expressed as the mean ± SEM for each group. The difference between groups was analyzed with a one-way, two-way, or repeated ANOVA, followed by the Bonferroni/Dunn multiple range-test. The Student *t*-test was used to compare two sets of data.

RESULTS

General Characteristics of Cyp $D^{-/-}$ Mice

The genotype for the Cyp D locus was assessed by PCR (Fig. 1A). Cyp $D^{-/-}$ mice were confirmed to lack Cyp D protein by Western blotting (Fig. 1B). Cyp $D^{-/-}$ mice were healthy and showed no changes in physical characteristics (body weight, or appearance of fur and whiskers) at 3 months (Fig. 1C). Although Luvisetto et al. (2008) have recently reported that Cyp $D^{-/-}$ mice show adult onset obesity, our mice did not show gross changes in physical characteristics, including body weight, with age (data not shown).

Histological Appearance of the Hippocampus in Cyp $D^{-/-}$ Mice

Strong immunoreactivity for Cyp D was observed in the granule cell layer and pyramidal cell layer in the hippocampus (Fig. 1D). In higher resolution image of CA1 regions, Cyp D immunoreactivity was localized in NeuN positive neuronal cells (Fig. 1E). With enhanced sensitivity of microscope, Cyp D immunoreactivity was also observed in astrocytes, though sparsely (Fig. 1E). No Cyp D protein was pressed in the brains of Cyp $D^{-/-}$ mice as confirmed by immunofluorescent staining (Fig. 1D). Nissl staining and immunostaining for the astrocyte marker GFAP showed neither gross structural abnormalities (Fig. 1D) nor any morphological abnormality of neuronal cells and astrocytes (Fig. 1F). The expression levels of the dendritic marker MAP2, neuronal growth cone marker GAP-43, presynaptic marker synaptophysin, and GFAP remained unchanged in hippocampal homogenates from Cyp $D^{-/-}$ mice as compared

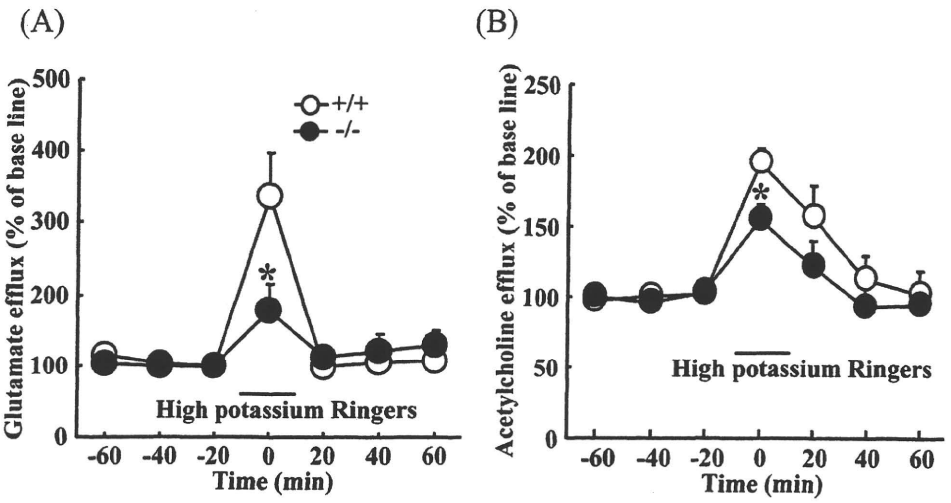

FIGURE 2. Deficiency of Cyclophilin D inhibits the release of glutamate and acetylcholine in the hippocampus. High potassium-evoked release of glutamate (A) and acetylcholine (B) from the hippocampus in the Cyp $D^{-/-}$ and wild type mice; High potassium-induced release of glutamate from the hippocampus was measured in the Cyp $D^{-/-}$ and wild-type mice. Values correspond to mean ± SEM (wild-type mice, $n = 6$; Cyp $D^{-/-}$ mice, $n = 7$). Results with repeated ANOVA were as follows: time, $F(3,33) = 11.36$, $P < 0.01$; Cyp D deficiency, $F(1,33) = 2.28$, $P = 0.16$; interaction time with Cyp D deficiency, $F(3,33) = 4.48$, $P < 0.01$. High potassium-induced release of acetylcholine from the hippocampus was measured in the Cyp $D^{-/-}$ mice. Values correspond to mean ± SEM (wild-type mice, $n = 10$; Cyp $D^{-/-}$ mice; $n = 11$). Results with repeated ANOVA were as follows: time, $F(3,57) = 11.54$, $P < 0.01$; Cyp D deficiency, $F(1,57) = 2.16$, $P = 0.16$; interaction of time with Cyp D deficiency, $F(3,57) = 0.45$, $P = 0.71$, $^*P < 0.05$ versus wild-type mice. +/+, wild-type mice; −/−, Cyp $D^{-/-}$ mice.

with those from wild-type mice (Fig. 1G; $n = 10$ per group; Student t-test).

Deficiency of Cyclophilin D Inhibits the Release of Glutamate and ACh in the Hippocampus

The release of neurotransmitters in the hippocampus plays an important role in learning and memory (Stefani and Gold, 2001; Mereu et al., 2003). Therefore, changes in the amounts of glutamate and ACh released in the hippocampus were investigated by microdialysis in the Cyp $D^{-/-}$ mice. The basal levels of glutamate in the hippocampus of the wild-type and Cyp $D^{-/-}$ mice were 0.55 ± 0.13 and 0.46 ± 0.21 pmol/10 µl/10 min, respectively (mean ± SEM; n = 6–7 per group). The amount of glutamate released in response to high potassium (50 mM) in the hippocampus was significantly lower in the Cyp $D^{-/-}$ mice than in the wild-type mice (Fig. 2A; repeated ANOVA, post hoc Bonferroni/Dunn multiple range-test, $P < 0.05$). The basal levels of ACh in the hippocampus of the wild-type and Cyp $D^{-/-}$ mice were 0.15 ± 0.04 and 0.17 ± 0.03 nmol/10 µl/10 min, respectively (mean ± SEM; n = 10–11 per group). The amount of ACh released in response to high potassium (50 mM) in the hippocampus was significantly lower in the Cyp $D^{-/-}$ mice than in the wild-type mice (Fig. 2B; $P < 0.05$). These results indicate that a deficiency of Cyp D results in inhibition of the potassium-induced release of glutamate and ACh in the hippocampus.

No Influence of the Cyclophilin D Deficiency on Glutamatergic and Cholinergic Nervous System-Related Protein Expression in the Hippocampus

As demonstrated above, Cyp $D^{-/-}$ mice showed a hypoglutamatergic and hypocholinergic response in the hippocampus in the presence of high potassium. It was possible that the deficiency in Cyp D affected the expression of these neuronal system-related proteins such as receptors, synthetases, degradation enzymes, and transporters. To test this possibility, the expression of NMDA receptor subunits, glutaminase (GLS), glutamate transporters, choline acetyltransferase (ChAT), and acetyltransferase (AChE), was analyzed by Western blotting. There was no significant difference in NR1, NR2A, NR2B, GLS, GLAST, GLT-1, ChAT, and AChE protein levels in the hippocampus between wild-type and Cyp $D^{-/-}$ mice (Fig. 3; n = 10 per group; Student t-test). These data show that the hypoglutamatergic and hypocholinergic responses observed in Cyp $D^{-/-}$ mice were not due to changes in expression levels of proteins involved in these neurotransmitters response.

Impairment by Cyclophilin D Deficiency of Learning and Memory

Spontaneous alternation in the Y-maze test

We evaluated short-term memory using a Y-maze test. There was no significant difference in the number of arm entries between the two groups (Fig. 4A; n = 16–17 per group; Student

Hippocampus

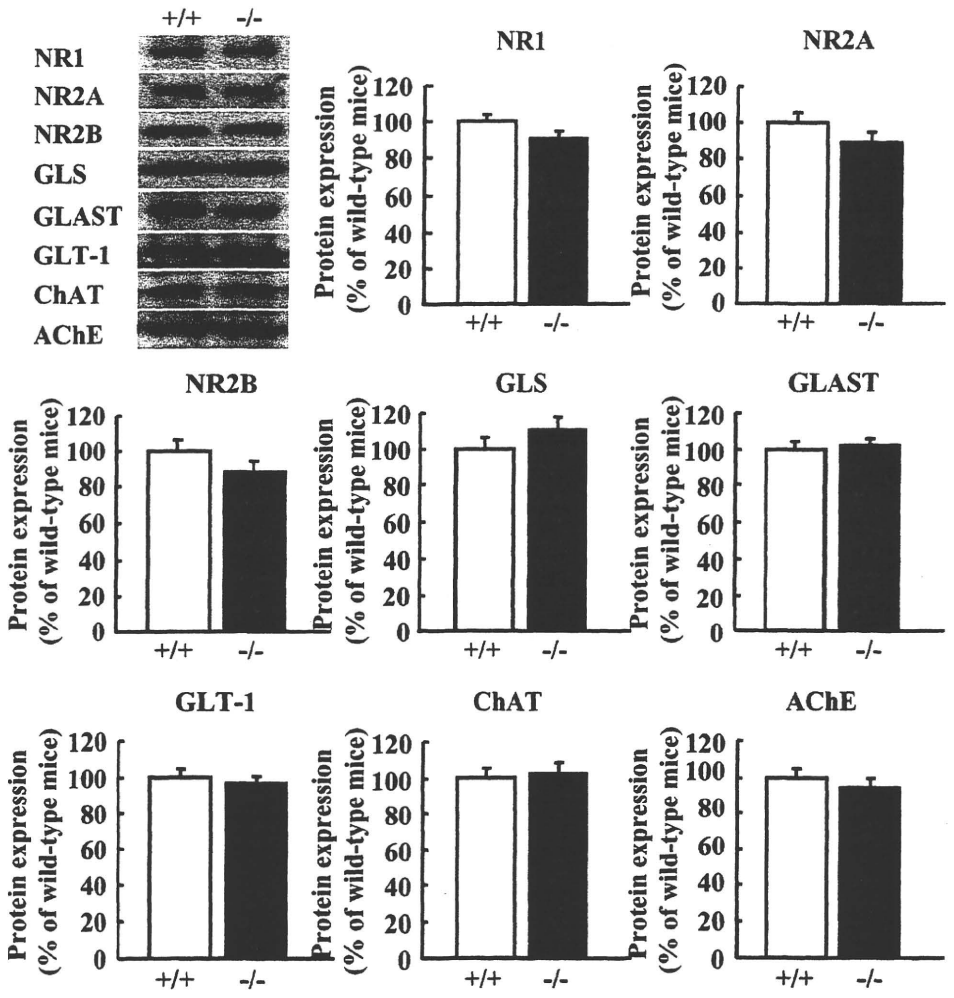

FIGURE 3. **No influence of Cyclophilin D deficiency on glutamatergic nervous system-related protein expression in the hippocampus. Western blot analysis of homogenates from the hippocampus of the Cyp $D^{-/-}$ and wild-type mice. No difference was observed between the two genotypes (wild-type mice, $n = 10$; Cyp $D^{-/-}$ mice, $n = 10$; Student t-test). NR1, NMDA receptor 1 subunit; NR2A, NMDA receptor 2A subunit; NR2B, NMDA receptor 2B subunit; GLS, glutaminase; GLAST, glutamate-aspartate transporter; GLT-1, glial glutamate transporter-1; ChAT, choline acetyltrasferase; AChE, acetylcholinesterase; +/+, wild-type mice; −/−, Cyp $D^{-/-}$ mice.**

t-test), suggesting that all mice have the same levels of motivation, curiosity, and motor function. However, Cyp $D^{-/-}$ mice showed significantly reduced spontaneous alternation behavior in the Y-maze compared with wild-type mice (Fig. 4B; $P < 0.05$), indicating an impairment of short-term memory.

Object recognition in the novel-object recognition test

We evaluated the visual recognition memory of Cyp $D^{-/-}$ mice using the novel-object recognition test. During the training session, there were no significant differences in exploratory preference between the two objects (Fig. 5A; $n = 16$–17 per group; repeated ANOVA, post hoc Bonferroni/Dunn multiple range-test) and the total time spent exploring both objects between the two groups (Fig. 5B), suggesting that all mice have

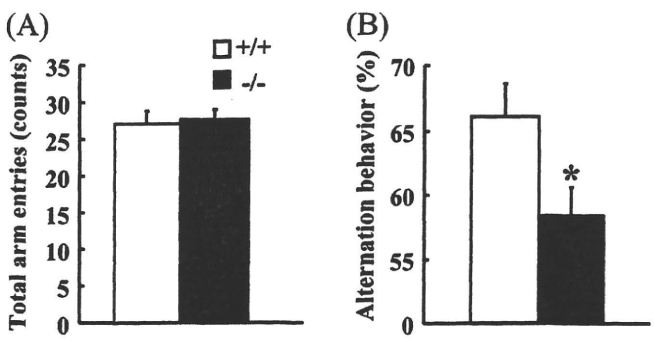

FIGURE 4. **Impairment of short-term memory by Cyclophylin D deficiency in the Y-maze test. (A) Total arm entries; (B) Alternation behavior. Percent alternation during an 8-min session in the Y-maze test was measured. Values indicate mean ± SEM (wild-type mice, $n = 17$; Cyp $D^{-/-}$ mice; $n = 16$). *$P < 0.05$ versus wild-type mice (Student t-test). +/+, wild-type mice; −/−, Cyp $D^{-/-}$ mice.**

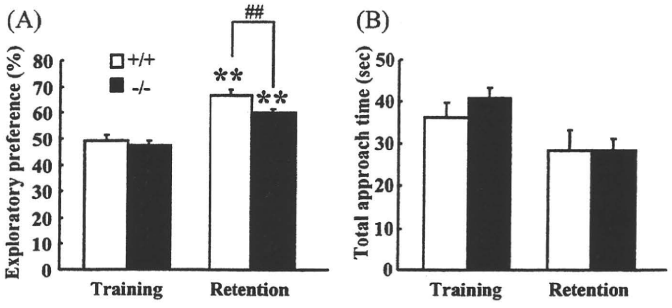

FIGURE 5. Impairment of object recognition memory by Cyclophylin D deficiency in the novel-object recognition test. (A) Exploratory preference; (B) Total approach time. The retention session was carried out 24 h after the training. Exploratory preference during a 10-min session in the novel-object recognition test was measured. Values indicate mean ± SEM (wild-type mice, n = 17; Cyp $D^{-/-}$ mice; n = 16). Results with the repeated ANOVA were as follows; exploratory preference: training/retention, $F(1,31)$ = 122.53, $P < 0.01$; Cyp D deficiency, $F(1,31)$ = 9.52, $P < 0.01$; interaction of training/retention with Cyp D deficiency, $F(1,31)$ = 2.22, P = 0.14; total approach time: training/retention, $F(1,31)$ = 28.32, $P < 0.01$; Cyp D deficiency, $F(1,31)$ = 0.62, P = 0.44; interaction of training/retention with Cyp D deficiency, $F(1,31)$ = 1.10, P = 0.30, $^{**}P < 0.01$ versus training. $^{\#\#}P < 0.01$ versus trained, wild-type mice. +/+, wild-type mice; −/−, Cyp $D^{-/-}$ mice.

the same levels of motivation, curiosity, and interest in exploring novel objects.

For the retention session, both groups of mice took longer time to explore the novel object than the familiar object (Fig. 5A, $P < 0.01$). However, the level of exploratory preference for the novel objects was significantly decreased in Cyp $D^{-/-}$ mice compared to wild-type mice (Fig. 5A, $P < 0.01$), indicating an impairment of visual recognition memory.

Reference memory in the Morris water maze test

We evaluated reference memory using the Morris water maze test. Both groups of mice managed to learn the position of the hidden platform (Fig. 6A). However, Cyp $D^{-/-}$ mice took significantly longer time and distance to reach the platform than wild-type mice (Fig. 6A; n = 16–17 per group; repeated ANOVA, post hoc Bonferroni/Dunn multiple range-test; $P < 0.01$), indicating an impairment of reference memory. When the probe test was carried out following the tenth block of training, wild-type mice searched preferentially in the trained quadrant (Fig. 6B; repeated ANOVA, post hoc Bonferroni/Dunn multiple range-test; $P < 0.01$), but Cyp $D^{-/-}$ mice did not. The decreased ability did not reflect a loss of swimming ability and motivation, because swimming speed and distance in the probe test were similar to those in wild-type mice (swimming speed; wild-type mice: 19.14 ± 0.78 cm/s, Cyp $D^{-/-}$ mice: 16.12 ± 1.33 cm/s, swimming distance; wild-type mice: 1,141 ± 47 cm, Cyp $D^{-/-}$ mice: 962 ± 80 cm).

Associative learning in the cued and contextual fear conditioning tests

We evaluated associative learning in the conditioned fear learning test. In the preconditioning phase, the mice of both groups hardly showed any freezing response, and there were no differences in basal levels of the freezing response between the groups (Figs. 7A,B; n = 16–17 per group; repeated ANOVA, post hoc Bonferroni/Dunn multiple range-test). In

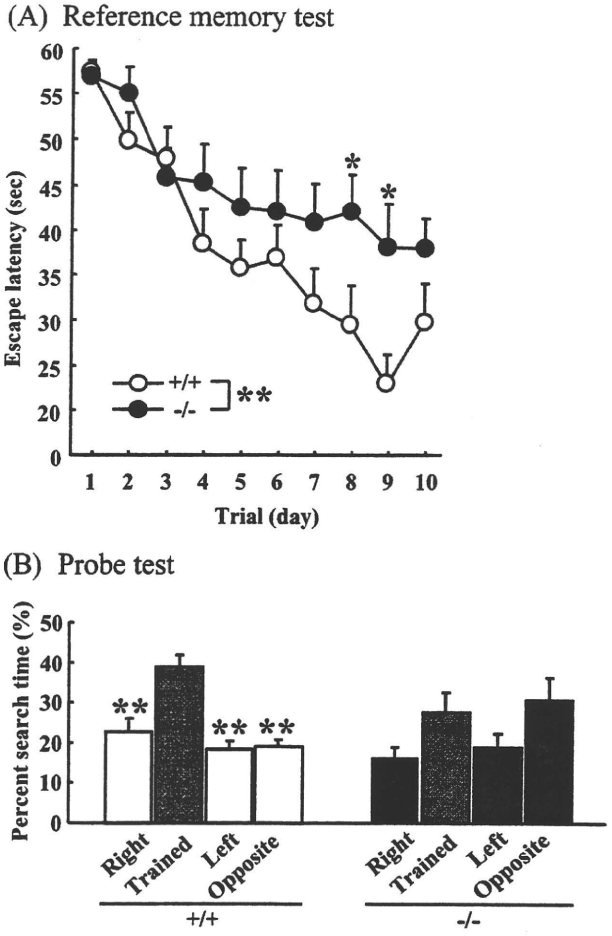

FIGURE 6. Impairment of reference memory by Cyclophylin D deficiency in the Morris water maze test. (A) Reference memory test. Escape latency during a 60-s session in the water maze test was measured. Values indicate mean ± SEM (wild-type mice, n = 17; Cyp $D^{-/-}$ mice; n = 16). Results with the repeated ANOVA were as follows: trial, $F(9,279)$ = 11.96, $P < 0.01$; animal group, $F(1,31)$ = 7.27, $P < 0.05$; interaction of trial with animal group, $F(9,279)$ = 1.13, P = 0.34. $^{**}P < 0.01$, $^{*}P < 0.05$ versus wild-type mice. (B) Probe test. The probe test was performed after training on day 10 in the Morris water maze test. Percent search time during a 60-s session in the water maze test was measured. Values indicate mean ± SEM (wild-type mice, n = 17; Cyp $D^{-/-}$ mice; n = 16). Results with the repeated ANOVA were as follows: quadrant, $F(3,93)$ = 5.57, $P < 0.01$; Cyp D deficiency, $F(1,31)$ = 0.01, P = 0.91; interaction of quadrant with Cyp D deficiency, $F(3,93)$ = 2.95, $P < 0.05$. $^{**}P < 0.01$ versus trained quadrant. +/+, wild-type mice; −/−, Cyp $D^{-/-}$ mice.

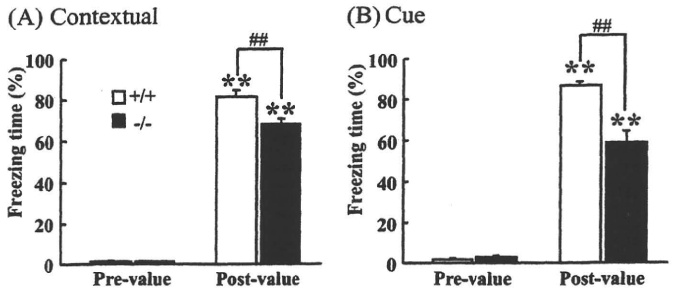

FIGURE 7. Impairment of associative learning by Cyclophylin D deficiency in the conditioned fear learning test. The test session was carried out 24 h after the conditioning. Context-dependent (A) and Cue-dependent (B) freezing times were measured. Values indicate mean ± SEM (wild-type mice, n = 17; Cyp $D^{-/-}$ mice; n = 16). Results with the repeated ANOVA were as follows; context-dependent test: conditioning, $F(1,31) = 1{,}127.89$, $P < 0.01$; Cyp D deficiency, $F(1,31) = 9.12$, $P < 0.01$; interaction of conditioning with Cyp D deficiency, $F(1,31) = 9.12$, $P < 0.01$; cue-dependent test: conditioning, $F(1,31) = 703.45$, $P < 0.01$; Cyp D deficiency, $F(1,31) = 17.14$, $P < 0.01$; interaction of conditioning with Cyp D deficiency, $F(1,31) = 29.96$, $P < 0.01$, $^{**}P < 0.01$ versus pre-conditioning. $^{\#\#}P < 0.01$ versus conditioned, wild-type mice. +/+, wild-type mice; −/−, Cyp $D^{-/-}$ mice.

the contextual learning test, both groups showed a marked contextual freezing response 24 h after fear conditioning (Fig. 7A; $P < 0.01$). However, Cyp $D^{-/-}$ mice exhibited less freezing response in the contextual tests (Fig. 7A; $P < 0.01$), indicating an impairment of associative learning. In the cued learning test, Cyp $D^{-/-}$ mice exhibited less freezing (Fig. 7B; $P < 0.01$), indicating an impairment of associative learning. Furthermore, no aberrant nociceptive responses to electric footshocks were observed in the Cyp $D^{-/-}$ mice: the footshock thresholds in the Cyp $D^{-/-}$ mice (flinching, 0.28 ± 0.02 mA; vocalizing, 0.62 ± 0.05 mA; jumping, 0.78 ± 0.08 mA) were the same as those in wild-type mice (flinching, 0.22 ± 0.03 mA; vocalizing, 0.77 ± 0.05 mA; jumping, 0.71 ± 0.11 mA).

Recapitulation of Cyclophilin D Deficiency by Infusion of Cyclosporine A Into the Hippocampus

To examine the role of hippocampal Cyp D in learning and memory, we microinjected CsA, an inhibitor of Cyp D, into the hippocampus, and evaluated its effect on performance in the novel-object recognition test and conditioned fear learning test. In the novel-object recognition test, the mice were microinjected with CsA (100 pmol/mouse/unilateral) 10 min before the training trial. During the training session, there were no significant differences in exploratory preference between the two objects and total exploratory time between the two groups (Figs. 8A,B; n = 8–9 per group; repeated ANOVA, post hoc Bonferroni/Dunn multiple range-test). However, the level of exploratory preference for the novel objects in mice treated with CsA was significantly decreased compared to that in mice treated with vehicle (Fig. 8A, $P < 0.05$), indicating a role for hippocampal Cyp D in this form of learning and memory. In the conditioned fear learning test, CsA was microinjected into the hippocampus 10 min before the conditioning trial. The mice treated with CsA exhibited less freezing response 24 h after fear conditioning in the contextual tests, which is known to be hippocampus-dependent (Fig. 8C; n = 16–17 per group; Student t-test; $P < 0.01$). But there was no difference in the cued freezing response 24 h after fear conditioning among the groups in the cued learning test, which is known to be hippocampus-independent (Fig. 8D). These results indicate that hippocampal Cyp D plays a role in the hippocampal-dependent form of learning and memory.

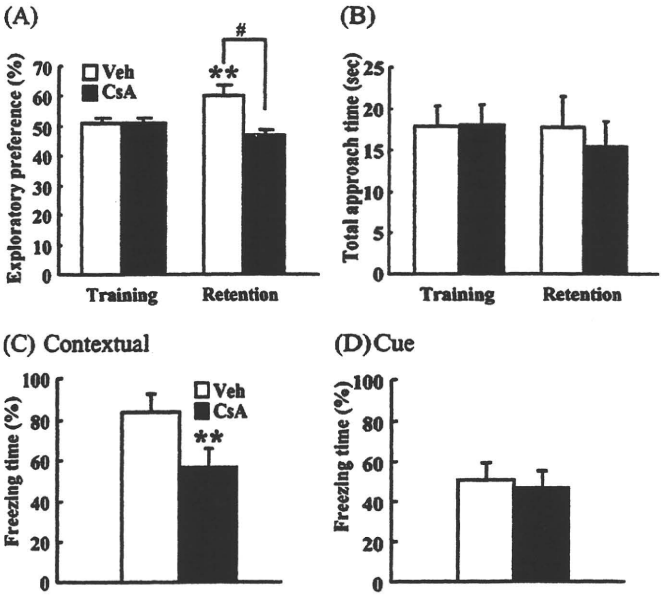

FIGURE 8. Recapitulation of Cyclophilin D deficiency by infusion of CsA into the hippocampus. Novel object recognition test: (A) Exploratory preference; (B) Total approach time. The retention session was carried out 24 h after the training. CsA (100 pmol/mouse/unilateral) was infused into the hippocampus 10 min before the training trial. Exploratory preference during a 10-min session in the novel-object recognition test was measured. Values indicate mean ± SEM (vehicle-treated mice, n = 9; CsA-treated mice, n = 8). Results with the repeated ANOVA were as follows; exploratory preference: training/retention, $F(1,15) = 2.67$, $P = 0.12$; treatment, $F(1,15) = 7.17$, $P < 0.05$; interaction training/retention with treatment, $F(1,15) = 12.83$, $P < 0.05$; total approach time: training/retention, $F(1,15) = 0.12$, $P = 0.64$; treatment, $F(1,15) = 0.06$, $P = 0.81$; interaction training/retention with treatment, $F(1,15) = 0.89$, $P = 0.36$. $^{**}P < 0.01$ versus training. $^{\#}P < 0.05$ versus trained, vehicle-treated mice. Conditioned fear learning test: The test session was carried out 24 h after the conditioning. Context-dependent (C) and cue-dependent (D) freezing times were measured. Values indicate mean ± SEM (vehicle-treated mice, n = 10; Cyclosporine A-treated mice, n = 10). $^{**}P < 0.01$ versus vehicle-treated mice (Student t-test). Veh, vehicle-treated mice; CsA, Cyclosporine A-treated mice.

DISCUSSION

In this study, we analyzed mice with a deficiency of Cyp D to define its role in cognitive functions. Our behavioral data showed that Cyp $D^{-/-}$ mice have subtle but significant impairments of short-term memory in the Y-maze test, visual recognition memory in the novel-object recognition test, reference memory in the water maze test, and associative learning in the conditioned fear learning test. It is unlikely that the impaired performance of Cyp $D^{-/-}$ mice in learning and memory tests is due to changes in motivation or sensorimotor function, since the motivation for each of these behavioral tests is different, and different skills are required for a good performance in each test. Actually, there were no differences in total arm entries in the Y-maze test, total time spent exploring objects in the novel object test, swimming speed in the Morris water maze test, and freezing response in the preconditioning phase and nociceptive response between the wild-type and Cyp $D^{-/-}$ mice.

Cyp D immunoreactivity is abundant in neuronal layers but sparse in astrocytes in the adult mouse brain. Naga et al. (2007) also showed that Cyp D is present at high levels in neurons and low levels in astrocytes in adult rat brain using immunohistochemistry and in primary rat neuron and astrocyte cultures using Western blotting. Although it is possible that Cyp D deficiency-induced developmental abnormalities in the neuronal and astrocytic architecture lead to cognitive dysfunctions, we did not observe histopathological abnormalities on Nissl staining and GFAP immunostaining or the irregular expression of neuronal (MAP2a-c, GAP-43, and synaptophysin) and glial (GFAP) marker proteins on Western blotting. Hippocampus as well as perirhinal and prefrontal cortex is crucial for recognition memory in the novel-object recognition test (Rampon et al., 2000; Winters and Bussey, 2005; Nagai et al., 2007). Reference memory in the Morris water maze test (Morris et al., 1982) and associative learning in the contextual, but not cued conditioned fear learning test (Phillips and LeDoux, 1992), are dependent on the hippocampus. Hippocampal infusion of CsA, an inhibitor of Cyp D (Halestrap and Davidson, 1990), replicated the hippocampus-dependent behavioral cognitive dysfunctions (impairments of recognition memory in the novel-object recognition test and of associative learning in the contextual test) observed in Cyp $D^{-/-}$ mice, except for the impairment of associative learning in the cued conditioned fear learning test, which is known to depend on the amygdala (Phillips and LeDoux, 1992). Taken together, these results strongly indicate that the role of Cyp D in cognitive functions is functional rather than developmental in nature.

Mitochondrial calcium buffering is an important regulator of synaptic function (Tang and Zucker, 1997; Billups and Forsythe, 2002). Recent studies have suggested that Cyp D-regulated MPT plays an important role in mitochondrial synaptic Ca^{2+} buffering, hippocampal synaptic plasticity, and learning and memory (Weeber et al., 2002; Levy et al., 2003; Naga et al., 2007). Mitochondria from synaptosomes, isolated from rat cerebral cortex, have less Ca^{2+} buffering ability than the nonsynaptic pool of mitochondria (Brown et al., 2006). This difference reflects the higher levels of Cyp D in synaptic than nonsynaptic mitochondria (Naga et al., 2007). The application of CsA, a deficiency of Cyp D, and a deficiency of VDAC all increase Ca^{2+} uptake capacity in isolated mitochondria (Levy et al., 2003; Naga et al., 2007). Interestingly, the application of CsA and a deficiency of VDAC impair paired-pulse facilitation and LTP (Weeber et al., 2002; Levy et al., 2003). The phenomena of paired pulse facilitation are generally accepted as a model of the presynaptic component of synaptic plasticity (Gottschalk et al., 1998). These results suggest that the cognitive dysfunction and impaired neurotransmission observed in Cyp $D^{-/-}$ mice is ascribable to deficiency of Cyp D-dependent MPT.

Excitatory transmitters such as ACh and glutamate change neural information processing by regulating the release of synaptic transmitters and modifying long-term synaptic plasticity (Giocomo and Hasselmo, 2007). In addition, the release of glutamate and ACh in hippocampus is related to cognitive performance in behavioral tests (Stefani and Gold, 2001; Mereu et al., 2003). In the present study, Cyp $D^{-/-}$ mice had lower extracellular glutamate and ACh levels in response to high potassium in the hippocampus than did the wild-type mice. Previously, a decrease in spontaneous extracellular glutamate release and increase in levels of the glutamate transporter GLAST were observed in schizophrenic animal models, which show impairments of memory (Mouri et al., 2007b; Murai et al., 2007). In present study, there was no difference in protein expression of neurotransmitter synthesis, metabolism and uptake in the glutamatergic and cholinergic neuronal system in hippocampus between wild-type and Cyp $D^{-/-}$ mice. Thus, it is unlikely that deficiency of Cyp D decrease glutamate and ACh response by modulation of these protein expressions of GLS, GLAST or GLT-1 between wild-type and Cyp $D^{-/-}$ mice. Although we have no detailed data about neurotransmitter levels in response to other potassium concentration, activities of neurotransmitters enzymes, and transporters in Cyp $D^{-/-}$ and hippocampal CsA-infused mice, our results along with other recent findings suggest that Cyp D and MPT play important roles in synaptic transmission.

Luvisetto et al. (2008) have reported that the Cyp $D^{-/-}$ mice generated by Basso et al. (2005) show adult onset obesity, increased anxiety/emotionality in the open field test and elevated plus maze test, and a facilitation of learning in the active and passive avoidance test at 10 months. As far as the obesity is concerned, we did not observe a significant difference in the body weight of Cyp $D^{-/-}$ mice up to 40 months, as compared with control littermates. We do not know the reason for this difference. Although our results are consistent with some of the results described by Luvisetto et al. (2008), notably that Cyp $D^{-/-}$ mice exhibited increased anxiety/emotionality in the elevated plus maze test (unpublished data), we did not observe any facilitation of learning and memory in our Cyp $D^{-/-}$ mice. It is conceivable that the avoidance behavior of Cyp $D^{-/-}$ mice is due to greater anxiety rather than greater learning ability. Du et al. (2008) have reported that the Cyp $D^{-/-}$ mice generated by Bains et al. (2005) show normal synaptic

plasticity and spatial memory in radial water maze test. These differences between Du's and our data might be due to different behavioral test, because the CypD$^{-/-}$ mice shows normal but slight increase of error in the behavior test at 6 months and decrease of long-term potentiation at 12–13 months (Du et al., 2008). More extensive investigation will be necessary to clarify these differences.

In summary, mice lacking Cyp D display cognitive dysfunction probably caused by the hypofunction of neurotransmission without developmental abnormalities. In pathological process, blockade of Cyp D could be a potent therapeutic strategy for degenerative disorders such as Alzheimer's disease, ischemia, and multiple sclerosis. It is possible that blockade of Cyp D impairs rather than facilitates cognitive function in normal condition. Our findings could contribute understanding not only the physiological roles of Cyp D in cognition but also appropriate use of Cyp D blocker for degenerative disorders.

REFERENCES

Baines CP, Kaiser RA, Purcell NH, Blair NS, Osinska H, Hambleton MA, Brunskill EW, Sayen MR, Gottlieb RA, Dorn GW, Robbins J, Molkentin JD. 2005. Loss of cyclophilin D reveals a critical role for mitochondrial permeability transition in cell death. Nature 434:658–662.

Basso E, Fante L, Fowlkes J, Petronilli V, Forte MA, Bernardi P. 2005. Properties of the permeability transition pore in mitochondria devoid of Cyclophilin D. J Biol Chem 280:18558–18561.

Bernardi P. 1999. Mitochondrial transport of cations: Channels, exchangers, and permeability transition. Physiol Rev 79:1127–1155.

Billups B, Forsythe ID. 2002. Presynaptic mitochondrial calcium sequestration influences transmission at mammalian central synapses. J Neurosci 22:5840–5847.

Brown MR, Sullivan PG, Geddes JW. 2006. Synaptic mitochondria are more susceptible to Ca2+overload than nonsynaptic mitochondria. J Biol Chem 281:11658–11668.

Crompton M, Virji S, Ward JM. 1998. Cyclophilin-D binds strongly to complexes of the voltage-dependent anion channel and the adenine nucleotide translocase to form the permeability transition pore. Eur J Biochem 258:729–735.

Dodge FA Jr, Rahamimoff R. 1967. Co-operative action a calcium ions in transmitter release at the neuromuscular junction. J Physiol 193:419–432.

Du H, Guo L, Fang F, Chen D, Sosunov AA, McKhann GM, Yan Y, Wang C, Zhang H, Molkentin JD, Gunn-Moore FJ, Vonsattel JP, Arancio O, Chen JX, Yan SD. 2008. Cyclophilin D deficiency attenuates mitochondrial and neuronal perturbation and ameliorates learning and memory in Alzheimer's disease. Nat Med 14:1097–1105.

Galat A. 1993. Peptidylproline *cis-trans*-isomerases: immunophilins. Eur J Biochem 216:689–707.

Giocomo LM, Hasselmo ME. 2007. Neuromodulation by glutamate and acetylcholine can change circuit dynamics by regulating the relative influence of afferent input and excitatory feedback. Mol Neurobiol 36:184–200.

Gottschalk W, Pozzo-Miller LD, Figurov A, Lu B. 1998. Presynaptic modulation of synaptic transmission and plasticity by brain-derived neurotrophic factor in the developing hippocampus. J Neurosci 18:6830–6839.

Halestrap AP, Davidson AM. 1990. Inhibition of Ca2(+)-induced large-amplitude swelling of liver and heart mitochondria by cyclosporin is probably caused by the inhibitor binding to mitochondrial-matrix peptidyl-prolyl *cis-trans*-isomerase and preventing it interacting with the adenine nucleotide translocase. Biochem J 268:153–160.

Halestrap AP, McStay GP, Clarke SJ. 2002. The permeability transition pore complex: Another view. Biochimie 84:153–166.

Kang JS, Tian JH, Pan PY, Zald P, Li C, Deng C, Sheng ZH. 2008. Docking of axonal mitochondria by syntaphilin controls their mobility and affects short-term facilitation. Cell 132:137–148.

Kokoszka JE, Waymire KG, Levy SE, Sligh JE, Cai J, Jones DP, MacGregor GR, Wallace DC. 2004. The ADP/ATP translocator is not essential for the mitochondrial permeability transition pore. Nature 427:461–465.

Lee D, Lee KH, Ho WK, Lee SH. 2007. Target cell-specific involvement of presynaptic mitochondria in post-tetanic potentiation at hippocampal mossy fiber synapses. J Neurosci 27: 13603–13613.

Leung AW, Halestrap AP. 2008. Recent progress in elucidating the molecular mechanism of the mitochondrial permeability transition pore. Biochim Biophys Acta 1777:946–952.

Levy M, Faas GC, Saggau P, Craigen WJ, Sweatt JD. 2003. Mitochondrial regulation of synaptic plasticity in the hippocampus. J Biol Chem 278:17727–17734.

Long AA, Kim E, Leung HT, Woodruff E 3rd, An L, Doerge RW, Pak WL, Broadie K. 2008. Presynaptic calcium channel localization and calcium-dependent synaptic vesicle exocytosis regulated by the Fuseless protein. J Neurosci 28:3668–3682.

Luvisetto S, Basso E, Petronilli V, Bernardi P, Forte M. 2008. Enhancement of anxiety, facilitation of avoidance behavior, and occurrence of adult-onset obesity in mice lacking mitochondrial cyclophilin D. Neuroscience 155:585–596.

Matsumoto S, Friberg H, Ferrand-Drake M, Wieloch T. 1999. Blockade of the mitochondrial permeability transition pore diminishes infarct size in the rat after transient middle cerebral artery occlusion. J Cereb Blood Flow Metab 19:736–741.

Mereu G, Fà M, Ferraro L, Cagiano R, Antonelli T, Tattoli M, Ghiglieri V, Tanganelli S, Gessa GL, Cuomo V. 2003. Prenatal exposure to a cannabinoid agonist produces memory deficits linked to dysfunction in hippocampal long-term potentiation and glutamate release. Proc Natl Acad Sci USA 100:4915–4920.

Morris RG, Garrud P, Rawlins JN, O'Keefe J. 1982. Place navigation impaired in rats with hippocampal lesions. Nature 297:681–683.

Morris RL, Hollenbeck PJ. 1993. The regulation of bidirectional mitochondrial transport is coordinated with axonal outgrowth. J Cell Sci 104:917–927.

Mouri A, Noda Y, Hara H, Mizoguchi H, Tabira T, Nabeshima T. 2007a. Oral vaccination with a viral vector containing Abeta cDNA attenuates age-related Abeta accumulation and memory deficits without causing inflammation in a mouse Alzheimer model. FASEB J 21:2135–2148.

Mouri A, Noda Y, Noda A, Nakamura T, Tokura T, Yura Y, Nitta A, Furukawa H, Nabeshima T. 2007b. Involvement of a dysfunctional dopamine-D1/*N*-methyl-D-aspartate-NR1 and Ca2+/calmodulin-dependent protein kinase II pathway in the impairment of latent learning in a model of schizophrenia induced by phencyclidine. Mol Pharmacol 71:1598–1609.

Murai R, Noda Y, Matsui K, Kamei H, Mouri A, Matsuba K, Nitta A, Furukawa H, Nabeshima T. 2007. Hypofunctional glutamatergic neurotransmission in the prefrontal cortex is involved in the emotional deficit induced by repeated treatment with phencyclidine in mice: implications for abnormalities of glutamate release and NMDA-CaMKII signaling. Behav Brain Res 180:152–160.

Muramatsu Y, Furuichi Y, Tojo N, Moriguchi A, Maemoto T, Nakada H, Hino M, Matsuoka N. 2007. Neuroprotective efficacy of FR901459, a novel derivative of cyclosporin A, in in vitro mitochondrial damage and in vivo transient cerebral ischemia models. Brain Res 1149:181–190.

Naga KK, Sullivan PG, Geddes JW. 2007. High cyclophilin D content of synaptic mitochondria results in increased vulnerability to permeability transition. J Neurosci 27:7469–7475.

Nagai T, Takuma K, Kamei H, Ito Y, Nakamichi N, Ibi D, Nakanishi Y, Murai M, Mizoguchi H, Nabeshima T, Yamada K. 2007. Dopamine D1 receptors regulate protein synthesis-dependent long-term recognition memory via extracellular signal-regulated kinase 1/2 in the prefrontal cortex. Learn Mem 14:117–125.

Nakagawa T, Shimizu S, Watanabe T, Yamaguchi O, Otsu K, Yamagata H, Inohara H, Kubo T, Tsujimoto Y. 2005. Cyclophilin D-dependent mitochondrial permeability transition regulates some necrotic but not apoptotic cell death. Nature 434:652–658.

Nicholls DG, Budd SL. 2000. Mitochondria and neuronal survival. Physiol Rev 80:315–360.

Norenberg MD, Rao KV. 2007. The mitochondrial permeability transition in neurologic disease. Neurochem Int 50:983–997.

Paxinos G, Franklin KBJ. 2004. The Mouse Brain in Stereotaxic Coordinates, Compact, 2nd ed. San Diego: Elsevier.

Phillips RG, LeDoux JE. 1992. Differential contribution of amygdala and hippocampus to cued and contextual fear conditioning. Behav Neurosci 106:274–285.

Rampon C, Tang YP, Goodhouse J, Shimizu E, Kyin M, Tsien JZ. 2000. Enrichment induces structural changes and recovery from nonspatial memory deficits in CA1 NMDAR1-knockout mice. Nat Neurosci 3:238–244.

Rowland KC, Irby NK, Spirou GA. 2000. Specialized synapse-associated structures within the calyx of Held. J Neurosci 20:9135–9144.

Schinzel AC, Takeuchi O, Huang Z, Fisher JK, Zhou Z, Rubens J, Hetz C, Danial NN, Moskowitz MA, Korsmeyer SJ. 2005. Cyclophilin D is a component of mitochondrial permeability transition and mediates neuronal cell death after focal cerebral ischemia. Proc Natl Acad Sci USA 102:12005–12010.

Shepherd GM, Harris KM. 1998. Three-dimensional structure and composition of CA3→CA1 axons in rat hippocampal slices: Implications for presynaptic connectivity and compartmentalization. J Neurosci 18:8300–8310.

Stefani MR, Gold PE. 2001. Intrahippocampal infusions of K-ATP channel modulators influence spontaneous alternation performance: Relationships to acetylcholine release in the hippocampus. J Neurosci 21:609–614.

Tang Y, Zucker RS. 1997. Mitochondrial involvement in post-tetanic potentiation of synaptic transmission. Neuron 118:483–491.

Weeber EJ, Levy M, Sampson MJ, Anflous K, Armstrong DL, Brown SE, Sweatt JD, Craigen WJ. 2002. The role of mitochondrial porins and the permeability transition pore in learning and synaptic plasticity. J Biol Chem 277:18891–18897.

Winters BD, Bussey TJ. 2005. Glutamate receptors in perirhinal cortex mediate encoding, retrieval, and consolidation of object recognition memory. J Neurosci 25:4243–4251.

Woodfield K, Rück A, Brdiczka D, Halestrap AP. 1998. Direct demonstration of a specific interaction between cyclophilin-D and the adenine nucleotide translocase confirms their role in the mitochondrial permeability transition. Biochem J 336:287–290.

Zoratti M, Szabò I. 1995. The mitochondrial permeability transition. Biochim Biophys Acta 1241:139–176.

Please cite this article in press as: Niwa et al., Knockdown of DISC1 by In Utero Gene Transfer Disturbs Postnatal Dopaminergic Maturation in the Frontal Cortex and Leads to Adult Behavioral Deficits, Neuron (2010), doi:10.1016/j.neuron.2010.01.019

Neuron
Article

Cell PRESS

Knockdown of DISC1 by In Utero Gene Transfer Disturbs Postnatal Dopaminergic Maturation in the Frontal Cortex and Leads to Adult Behavioral Deficits

Minae Niwa,[1,2,3,11] Atsushi Kamiya,[1,11] Rina Murai,[2,4] Ken-ichiro Kubo,[5] Aaron J. Gruber,[6] Kenji Tomita,[5] Lingling Lu,[2] Shuta Tomisato,[7] Hanna Jaaro-Peled,[1] Saurav Seshadri,[1] Hideki Hiyama,[1] Beverly Huang,[1] Kazuhisa Kohda,[7] Yukihiro Noda,[8] Patricio O'Donnell,[6] Kazunori Nakajima,[5] Akira Sawa,[1,9,*] and Toshitaka Nabeshima[2,4,10,*]

[1]Department of Psychiatry and Behavioral Sciences, Johns Hopkins University School of Medicine, Baltimore, MD 21287, USA
[2]Department of Chemical Pharmacology, Meijo University, Nagoya 4688503, Japan
[3]Department of Psychiatry
[4]Department of Neuropsychopharmacology and Hospital Pharmacy
Nagoya University Graduate School of Medicine, Nagoya 4668560, Japan
[5]Department of Anatomy, Keio University School of Medicine, Tokyo 1608582, Japan
[6]Department of Anatomy and Neurobiology, University of Maryland School of Medicine, Baltimore, MD 21201, USA
[7]Department of Physiology, Keio University School of Medicine, Tokyo 1608582, Japan
[8]Division of Clinical Science and Neuropsychopharmacology, Meijo University, Nagoya 4688503, Japan
[9]Department of Neuroscience, Johns Hopkins University School of Medicine, Baltimore, MD 21287, USA
[10]The Academic Frontier Project for Private Universities, Comparative Cognitive Science Institutes, Nagoya 4688503, Japan
[11]These authors contributed equally to this work
*Correspondence: asawa1@jhmi.edu (A.S.), tnabeshi@ccmfs.meijo-u.ac.jp (T.N.)
DOI 10.1016/j.neuron.2010.01.019

SUMMARY

Adult brain function and behavior are influenced by neuronal network formation during development. Genetic susceptibility factors for adult psychiatric illnesses, such as Neuregulin-1 and Disrupted-in-Schizophrenia-1 (DISC1), influence adult high brain functions, including cognition and information processing. These factors have roles during neurodevelopment and are likely to cooperate, forming pathways or "signalosomes." Here we report the potential to generate an animal model via in utero gene transfer in order to address an important question of how nonlethal deficits in early development may affect postnatal brain maturation and high brain functions in adulthood, which are impaired in various psychiatric illnesses such as schizophrenia. We show that transient knockdown of DISC1 in the pre- and perinatal stages, specifically in a lineage of pyramidal neurons mainly in the prefrontal cortex, leads to selective abnormalities in postnatal mesocortical dopaminergic maturation and behavioral abnormalities associated with disturbed cortical neurocircuitry after puberty.

INTRODUCTION

Adult brain function and behavior are influenced by neuronal network formation during development. Consequently, disturbances of brain development are suggested to underlie the pathology of adult mental disorders, such as schizophrenia and mood disorders (Lewis and Levitt, 2002; Rapoport et al., 2005; Savitz and Drevets, 2009; Tenyi et al., 2009). Consistent with this notion, genetic susceptibility factors for these disorders that have been recently identified, including Neuregulin-1 and Disrupted-in-Schizophrenia-1 (DISC1), have roles during neurodevelopment and are likely to cooperate, forming molecular "pathways" (Harrison and Weinberger, 2005; Jaaro-Peled et al., 2009; Owen et al., 2005). Furthermore, many studies have indicated that variations of these disease susceptibility genes influence high brain functions, including cognition and information processing, in both normal subjects and patients (Kéri, 2009; Krug et al., 2008; Tomppo et al., 2009). Thus, these genetic factors are believed to be good probes to explore mechanistic links between brain development and adult brain functions.

Schizophrenia is a debilitating disorder with onset in young adulthood, although many lines of evidence have indicated that pre- and perinatal brain disturbances underlie the initial risks for the disease (Buka and Fan, 1999; McNeil, 1995). It is possible that these initial risks may in turn affect postnatal brain maturation, resulting in the delayed onset of the disorder. Prodromal stages of schizophrenia in adolescence and young adulthood may reflect the dynamic pathophysiology of disturbed brain maturation (Cannon et al., 2003; Jaaro-Peled et al., 2009; White et al., 2006). Some excellent longitudinal studies with clinical subjects have attempted to address this question (White et al., 2006). Nonetheless, good animal models that can depict the sequential changes from the initial disturbances in early brain development to defects of postnatal brain maturation, leading to adult brain dysfunction associated with schizophrenia, are awaited to permit dissection and understanding of the molecular mechanisms during the course of disease progression. Mice with manipulations of genetic susceptibility factors for the disease may provide this opportunity (Chen et al., 2006). Once available, such models may shed light on the pathological

Please cite this article in press as: Niwa et al., Knockdown of DISC1 by In Utero Gene Transfer Disturbs Postnatal Dopaminergic Maturation in the Frontal Cortex and Leads to Adult Behavioral Deficits, Neuron (2010), doi:10.1016/j.neuron.2010.01.019

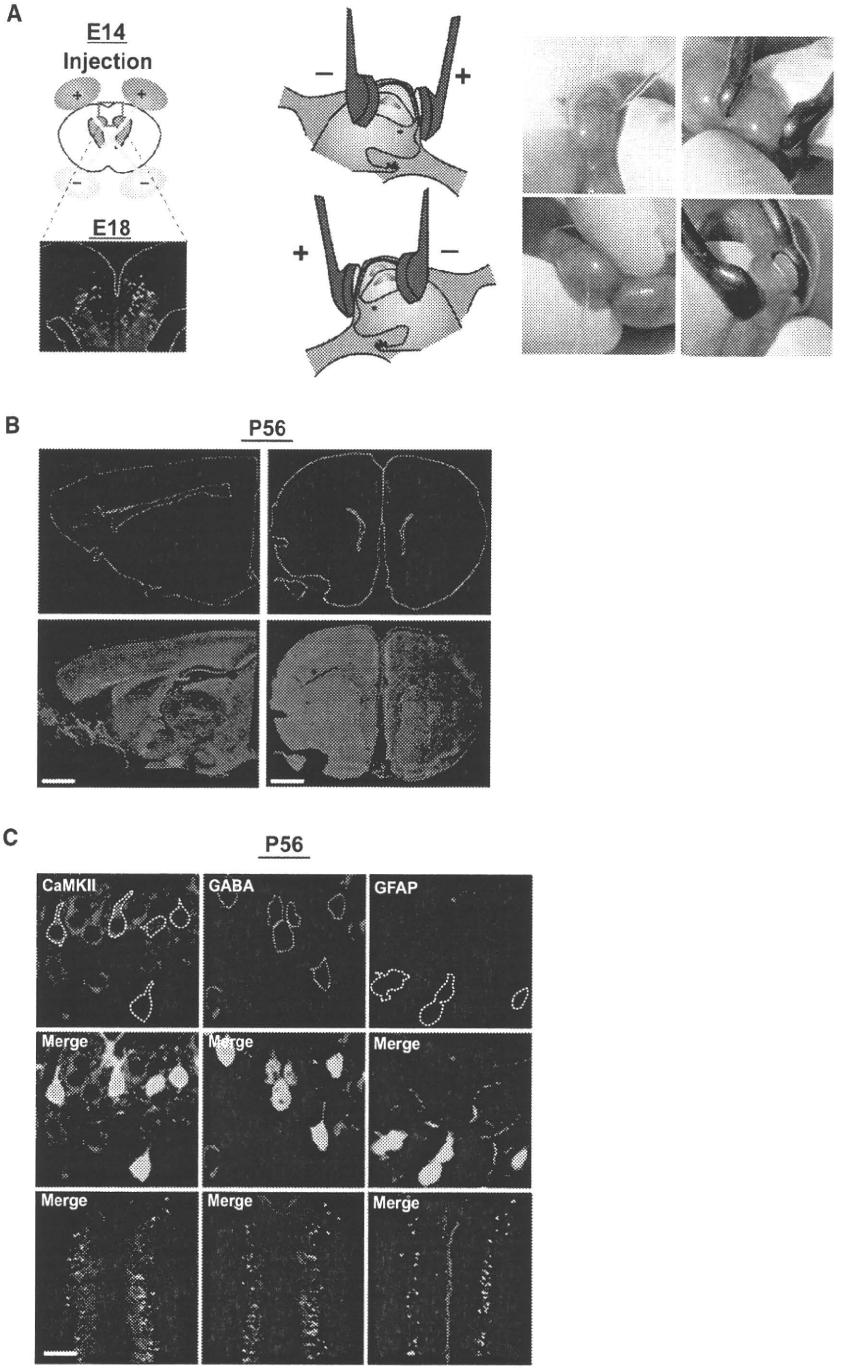

Figure 1. Selective Targeting of Constructs to Cells in a Lineage of Pyramidal Neurons in the Prefrontal Cortex via In Utero Gene Transfer

(A) Schematic representation of bilateral in utero injection of constructs followed by their incorporation by electroporation into progenitor cells in the ventricular zone at embryonic day 14 (E14). Migrating cells with GFP are visualized at E18 after injection of a GFP expression construct.

(B) Representative coronal and sagittal images of brains with GFP expression at P56 after injection of a GFP expression construct at E14. Blue, nucleus. The scale bars represent 1 mm.

(C) GFP-positive neurons in layers II/III at postnatal day 56 (P56) in mPFC. Most cells with GFP expression are CaMKII-positive pyramidal neurons (red in left panels), but not GABA (red in middle panels) or GFAP positive (red in right panels) at P56. The scale bar represents 100 μm.

mechanisms for schizophrenia. Furthermore, even more importantly, these models may clarify how minor or nonlethal brain disturbances in early development, possibly related to a combination of genetic variations, may affect high brain functions in adults, including cognition and information processing, in a wide range of mental conditions and even in subjects who may not be classified as having psychiatric disorders as defined by the Diagnostic and Statistical Manual of Mental Disorders.

Here we provide evidence to support the feasibility of in utero gene transfer to produce mouse models to address this question. In the present study, by utilizing this technique, we generated mice in which selective knockdown of DISC1 is achieved in a lineage for pyramidal neurons mainly in the prefrontal cortex (PFC), but only during development, which leads to maturation-dependent deficits in mesocortical dopaminergic projections and associated behavioral changes, including those in information processing and cognition.

RESULTS

Application of In Utero Gene Transfer to Modulate Expression of Target Genes in the Prefrontal Cortex

To evaluate the feasibility of the in utero gene transfer technique to analyze the modulation of gene expression in the PFC, an expression construct of green fluorescent protein (GFP) was injected into bilateral lateral ventricles and incorporated by electroporation into progenitor cells in the ventricular zone at embryonic day 14 (E14) in mice (Figure 1A; see Figure S1A available online). We analyzed sagittal and serial coronal sections from six randomly selected brains at postnatal day 56 (P56), and found that GFP-positive cells were located at +2.34 mm to ~+0.98 mm relative to Bregma, especially in the dorsolateral prefrontal cortex (DLPFC), medial prefrontal cortex (mPFC), orbitofrontal cortex (OFC), and anterior cingulate cortex (Figures 1B, S1B, and S1C). Thus, this method allows for gene targeting mainly into

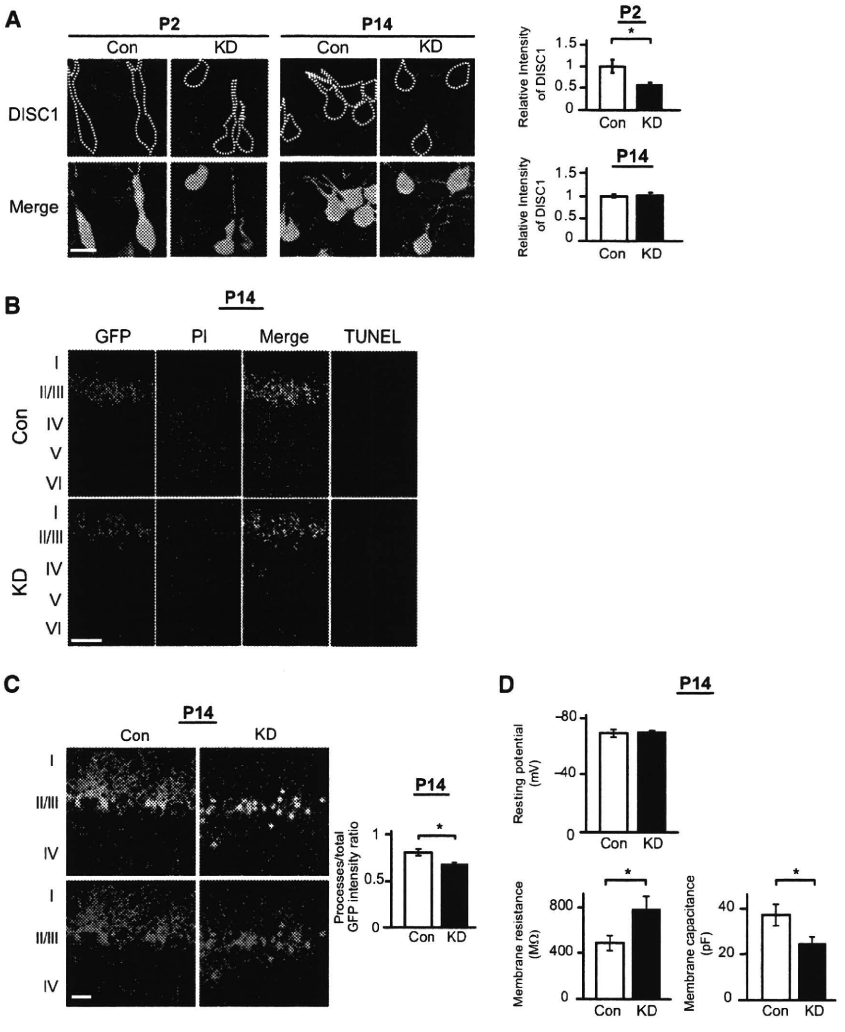

Figure 2. Mice with Knockdown of DISC1 in Pyramidal Neurons of the Prefrontal Cortex during Early Development via In Utero Gene Transfer Display Dendritic Abnormalities at P14

(A) Suppression of DISC1 immunoreactivity (red) in GFP-positive neurons is observed at P2, but not at P14, when shRNA to DISC1 is introduced (DISC1 knockdown [KD]) at E14 (*$p < 0.05$). A total of 30 GFP-positive cells from cortical slices of three DISC1 KD mice and those of three control mice with scrambled/control shRNA was analyzed and compared. The scale bar represents 10 μm.

(B) GFP-positive neurons with RNAi at layers II/III at P14 after injection at E14. KD mice display dendritic pathology without signs of apoptosis (TUNEL), consistent with our previous publication (Kamiya et al., 2005). Red, nucleus. The scale bar represents 100 μm.

(C) Reduction of GFP fluorescence intensity in dendrites relative to total GFP fluorescence intensity in mPFC of KD mice at P14, compared to those of Con mice (*$p < 0.05$, $n = 5$ per condition), suggesting impaired dendritic formation in KD mice. Red, nucleus. The scale bar represents 50 μm.

(D) Electrophysiological characteristics of pyramidal neurons with knockdown of DISC1 (majority of green cells) at layers II/III in mPFC at P14. Membrane resistance at −80 mV and membrane capacitance of GFP-positive neurons in DISC1 KD mice are significantly different compared with those in Con mice (*$p < 0.05$), whereas there is no difference in resting potential in these two groups ($n = 5$ per condition).

Data are expressed as mean ± SEM.

the PFC. In the developing cerebral cortex, pyramidal neurons migrate radially from the ventricular zone, whereas interneurons migrate tangentially from ganglionic eminence into the developing cerebral wall (Anderson et al., 1997; Marin and Rubenstein, 2003). Glial lineages originating from the subventricular zone are produced at late embryonic and early postnatal days (E17 to P14) (Sauvageot and Stiles, 2002). Therefore, the constructs are likely to be integrated into cells in a lineage of pyramidal neurons. Indeed, GFP-positive cells were confined only to pyramidal neurons, around 20% of which were GFP positive in layers II/III at P56 (Figure 1C). These results indicate that in utero gene transfer can be used for modulating target gene expression mainly in pyramidal neurons in PFC during brain development.

Transient Knockdown of DISC1 in PFC during Development via In Utero RNAi Transfer

In this study, we used DISC1 as a probe to address how molecular disturbance in cells of the pyramidal neuron lineage in PFC during early development might influence postnatal brain maturation and adult phenotypes. Thus, we injected a well-characterized DISC1 short-hairpin RNA (shRNA) together with a GFP expression construct at E14 according to the protocol described above, and confirmed targeting to PFC. Histological phenotypes in the developing cortex elicited by this shRNA (defects in neuronal progenitor proliferation, delay in neuronal migration, and resultant changes in arborization) are consistent with those elicited by other shRNAs to DISC1 thus far reported (Kamiya et al., 2005; Mao et al., 2009), and are rescued by overexpression of wild-type DISC1 ($DISC1^R$) (Figure S2A). Suppression of DISC1 seems to be transient, confirmed by knockdown of DISC1 for at least 7 days after injection, but not after 3 weeks (Figure 2A). In the present study, we have characterized the DISC1 knockdown-elicited phenotypic changes at P14 in greater detail, by extending our previous observation (Kamiya et al., 2005). As the result of the transient *knockdown* of DISC1 via RNA interference (RNAi) (designated DISC1 KD in this manuscript), GFP-positive pyramidal neurons were found in layers II/III without signs of apoptosis and with abnormal dendritic morphology (Figures 2B, 2C, and S2B–S2D). Impaired dendritic development in layers II/III at P14 in DISC1 KD mice was also functionally confirmed by electrophysiological approaches (Figure 2D).

Please cite this article in press as: Niwa et al., Knockdown of DISC1 by In Utero Gene Transfer Disturbs Postnatal Dopaminergic Maturation in the Frontal Cortex and Leads to Adult Behavioral Deficits, Neuron (2010), doi:10.1016/j.neuron.2010.01.019

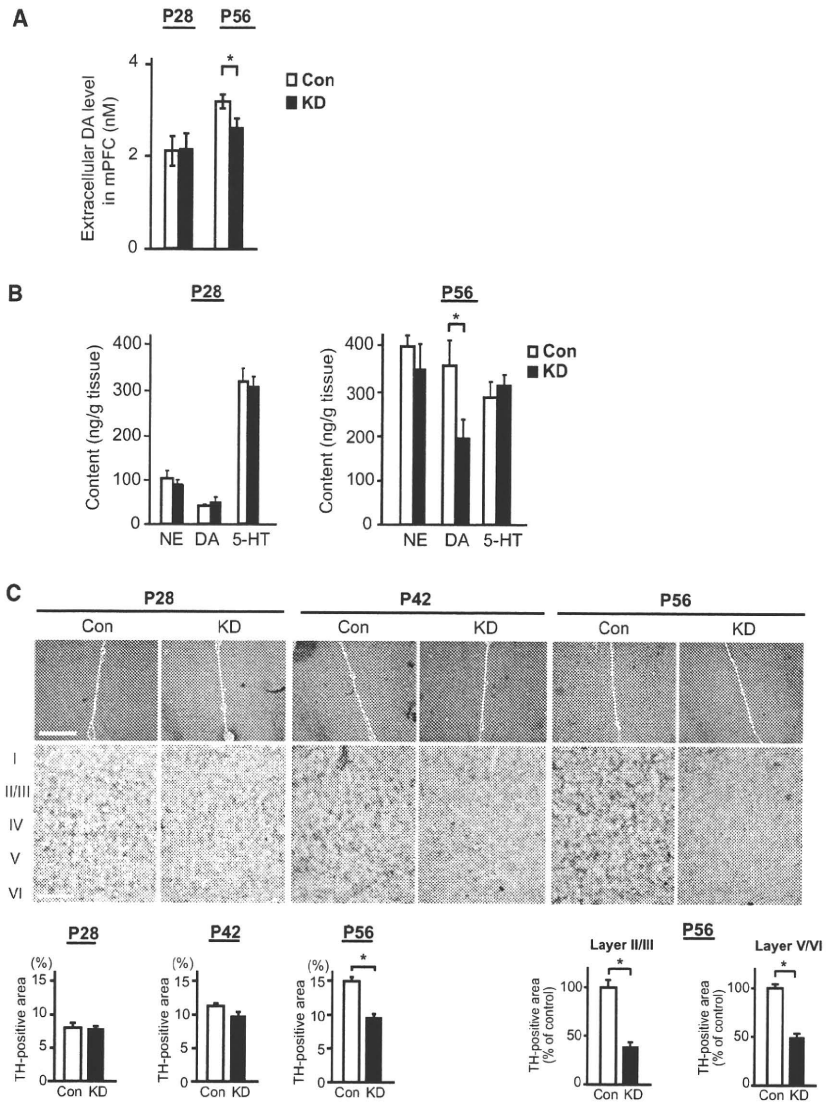

Figure 3. Disturbance in Postnatal Maturation of Mesocortical Dopaminergic Projections to the Medial Prefrontal Cortex in DISC1 Knockdown Mice

(A) Basal levels of extracellular dopamine (DA) in mPFC were analyzed by in vivo microdialysis, and a decrease in DISC1 KD mice compared with that in Con mice was detected at P56, but not at P28 (*$p < 0.05$, $n = 6$ per condition).

(B) Monoamine content in the frontal cortex as measured by HPLC. The level of DA in FC is decreased in DISC1 KD mice compared with that in Con mice at P56, but not at P28 (*$p < 0.05$, $n = 7$ per condition). No difference in the levels of NE and 5-HT is observed at these two time points.

(C) Immunostaining of tyrosine hydroxylase (TH) in mPFC, including prelimbic and infralimbic cortex (upper panels, low magnification; bottom panels, high magnification). TH level in mPFC is relatively decreased in KD mice compared with Con mice at P56 (*$p < 0.05$, $n = 6$ per condition) in both layers II/III and V/VI, whereas there is no difference between KD and Con at P28 and P42. The scale bar in low-magnification pictures represents 200 μm, and in high-magnification pictures represents 500 μm.

Data are expressed as mean ± SEM.

Disturbance in Postnatal Maturation of Mesocortical Dopaminergic Projections and Interneurons to the Medial Prefrontal Cortex in DISC1 KD Mice

Next, we addressed whether the dendritic abnormalities at P14 elicited by transient knockdown of DISC1 in the pre-/perinatal stages may later influence postnatal brain maturation. We first examined differences in body weight between DISC1 KD and control mice at P14, P28, and P56, which may reflect atypical developmental trajectories and could potentially affect maturation of neuronal circuits and behavior nonspecifically, but no difference in body weight was observed between these two groups (Figure S3A). At the histological level, we did not find any robust differences in Nissl staining in mPFC at P28 and P56 (Figure S3B). No difference between DISC1 KD and controls in immunostaining and western blotting for glial fibrillary acidic protein (GFAP) indicated that there was no gliosis in DISC1 KD mice at P28 and P56 (Figures S3C and S3D).

In contrast, we observed a marked decrease in the extracellular levels of dopamine in mPFC, measured by microdialysis, and total content of dopamine between KD and controls in FC at P56 but not at P28 (Figures 3A and 3B), whereas no changes were observed in total content of dopamine in other brain areas including nucleus accumbens, hippocampus, and cerebellum (Figure S3E). This change may be specific to dopamine, as no changes in glutamate, norepinephrine (NE), or serotonin were observed (Figure 3B, S3E, and S3F). Increase in the level of dopamine from birth to adolescence in the frontal cortex is known to reflect physiological maturation of the dopaminergic projection (Benes et al., 2000; Goto and Grace, 2007; Rosenberg and Lewis, 1995). Insufficient elevation of dopamine at P56 in DISC1 KD mice may indicate disturbed maturation of dopaminergic neurons. Consistent with this idea, relative immunoreactivity against tyrosine hydroxylase (TH), a marker of mature axon terminals of the dopaminergic projection, was decreased in both layers II/III and V/VI at P56, but not at P28 and P42, in DISC1 KD compared to control mice (Figure 3C). This relative decrease of TH was also confirmed by western blotting (Figure S3G). In contrast, we did not observe changes in expression of dopamine receptor-1 (D1R) and -2 (D2R) (Figures S3G and S3H).

Given that there are inter- and intralaminar connections of pyramidal neurons and GABAergic interneurons in local circuits in PFC where mesocortical dopaminergic neurons also have synaptic contact (Sesack et al., 2003), this aberrant development

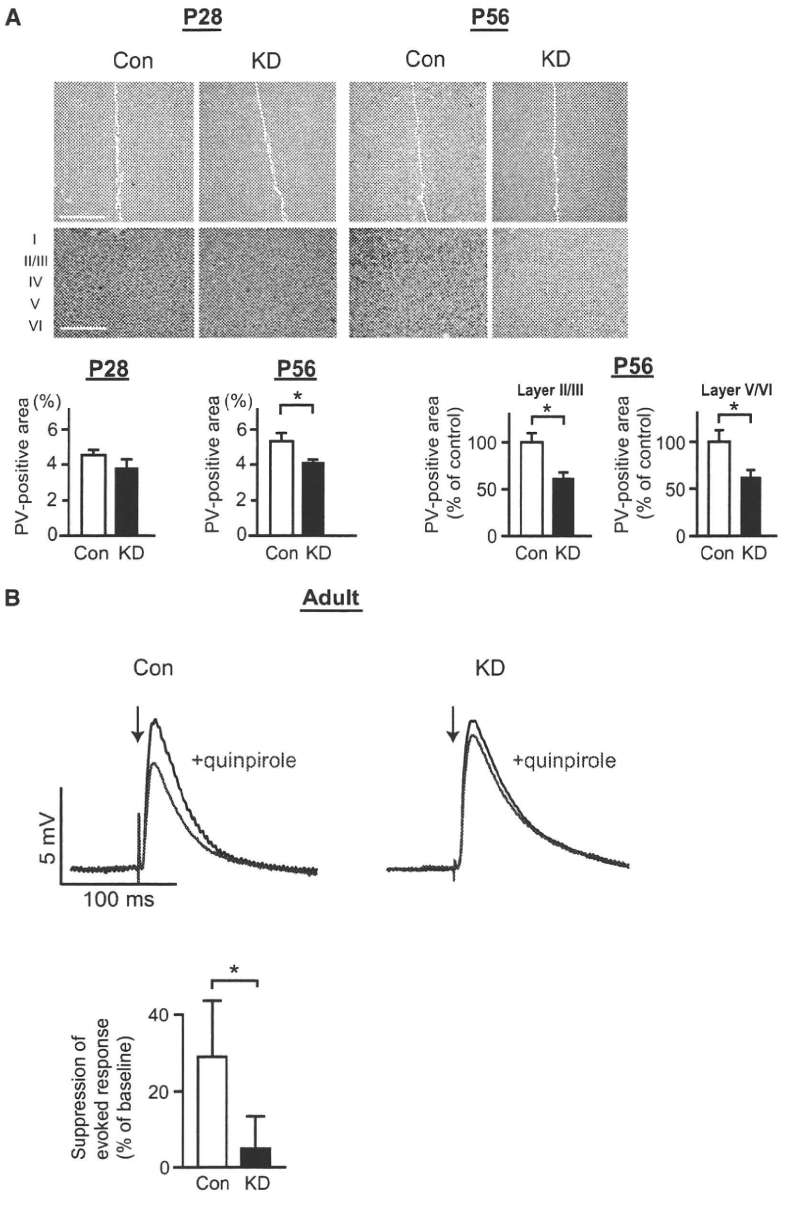

Figure 4. Disturbances of Interneurons and Pyramidal Neurons in PFC of DISC1 KD Mice after Puberty

(A) Immunostaining of parvalbumin (PV) in the mPFC (upper panels, low magnification; bottom panels, high magnification). Immunoreactivity of PV is quantified under each condition (lower graphs). The expression levels of PV in the mPFC (both layers II/III and V/VI) are decreased in KD mice compared with Con mice at P56, but not at P28 (*$p < 0.05$, $n = 6$ per condition). The scale bar in low-magnification pictures represents 200 μm, and in high-magnification pictures represents 500 μm.

(B) Electrophysiological responses of PFC pyramidal neurons to electrical stimulation recorded using the whole-cell patch-clamp technique in acute slices from young adult male mice. Overlay of membrane potential responses evoked with electrical stimulation of cortico-cortical fibers before (black trace) and during (red trace) bath application of the D2 dopamine agonist quinpirole (5 μM) in KD and Con mice. Arrows indicate times of single-pulse stimulation. Quinpirole attenuation of evoked excitatory postsynaptic potentials is reduced in KD mice (*$p < 0.05$, $n = 5$ per condition).

Data are expressed as mean ± SEM.

of the pyramidal neurons may affect GABAergic interneurons. To test this possibility, we examined the expression level of parvalbumin, a marker of the fast-spiking GABAergic interneurons. We observed reduction of parvalbumin immunoreactivity in layers II/III and V/VI in mPFC in DISC1 KD mice at P56 but not at P28, suggesting that there is a possible deficit of interneurons in adulthood; this effect is likely to occur during postnatal brain maturation (Figure 4A). To test whether dopamine regulation of local circuit processing in mPFC is altered in adult DISC1 KD mice, we recorded deep-layer pyramidal neurons by using the whole-cell patch-clamp technique in acute brain slices (Figure S4). Neither resting membrane potential nor input resistance was different from controls, indicating that basic somatic electrophysiological properties are not grossly disrupted in adult DISC1 KD mice (data not shown). Nonetheless, bath application of the D2R dopamine receptor agonist quinpirole attenuated electrically evoked membrane responses in control mice, but such attenuation was markedly reduced in DISC1 KD mice (Figure 4B). Taken together, these results suggest that neonatal pyramidal neuron deficits elicited by pre-/perinatal knockdown of DISC1 lead to overall disturbances in circuitry involving dopamine neurons, pyramidal neurons, and interneurons, manifested only after puberty.

Behavioral Deficits in DISC1 KD Mice after Puberty

We then questioned whether such neurochemical and physiological disturbance in postnatal brain maturation might result in behavioral deficits. Prepulse inhibition (PPI) reflects sensory gating function, a major indicator of information processing involving the cortex, which is also frequently impaired in various mental illnesses (Arguello and Gogos, 2006). DISC1 KD mice at P56, but not at P28, displayed decreased PPI, in comparison with controls (Figure 5A). DISC1-associated PPI deficits are further confirmed in mice by another shRNA to DISC1 that knocks down this molecule to a lesser extent than does the shRNA mainly used in this study (Kamiya et al., 2005, 2008; Mao et al., 2009): milder deficits in PPI that were consistent with the milder effect on DISC1 expression were observed in the mice (Figure S5A). We also tested the effect of clozapine, which is reported to elevate dopamine levels via blocking the D2 autoreceptor (Rayevsky et al., 1995). Very interestingly, when we administered clozapine acutely to DISC1 KD mice, we observed

Please cite this article in press as: Niwa et al., Knockdown of DISC1 by In Utero Gene Transfer Disturbs Postnatal Dopaminergic Maturation in the Frontal Cortex and Leads to Adult Behavioral Deficits, Neuron (2010), doi:10.1016/j.neuron.2010.01.019

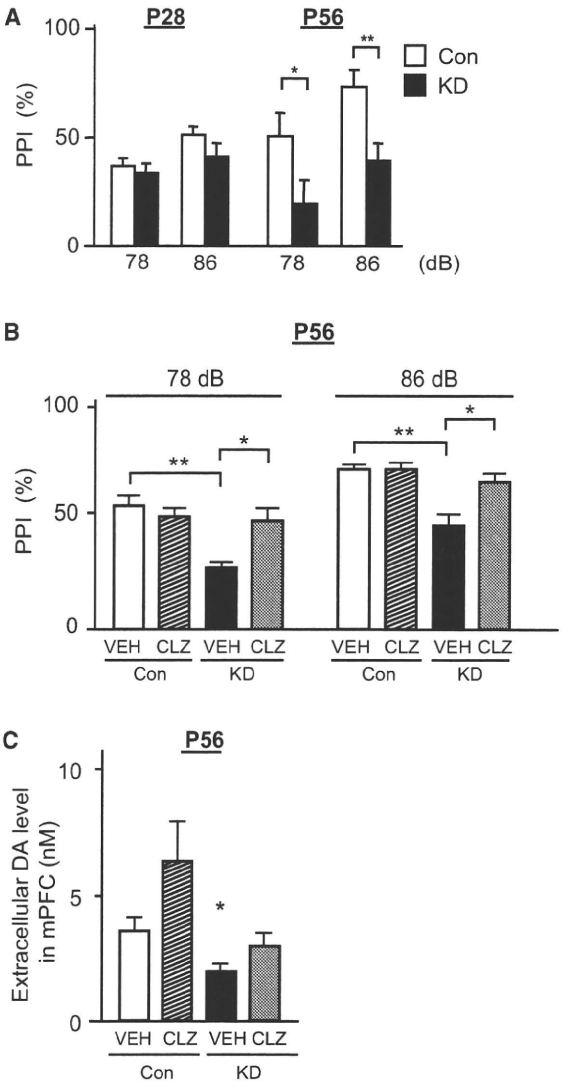

Figure 5. Attenuation of Prepulse Inhibition Deficits by Treatment with Clozapine in DISC1 KD Mice after Puberty

(A) Performance in prepulse inhibition (PPI) at P28 and P56. Impairment of PPI is observed in DISC1 KD mice at P56, but not at P28 (*$p < 0.05$, **$p < 0.01$, $n = 12$ per condition).

(B) Effect of clozapine (CLZ) on the impairment of PPI in KD mice at P56. Treatment with CLZ (3 mg/kg, i.p.) ameliorates the impairment of PPI in KD mice at P56 (*$p < 0.05$, **$p < 0.01$, $n = 16$ per condition). VEH, vehicle.

(C) Effect of CLZ on extracellular DA levels in mPFC by in vivo microdialysis. Administration of CLZ (3 mg/kg, i.p.) elevates extracellular DA levels in mPFC in both Con and KD mice at P56 (*$p < 0.05$, $n = 4$ per condition).

Data are expressed as mean ± SEM.

normalized levels of dopamine in mPFC and improvement of PPI deficits, without alterations in the startle amplitude (Figures 5B, 5C, S5B, and S5C). These results suggest that PPI deficits in DISC1 KD mice are, at least in part, associated with decreased levels of dopamine in the mPFC at P56.

The novel object recognition task (NORT) measures functions of the hippocampus and the cortex, including functions associated with visual working memory (Ozawa et al., 2006). No difference was observed in exploratory preference during the training between control and KD mice, suggesting that there were no significant differences in curiosity and/or motivation to explore objects between the two groups (Figure S5D). In contrast, KD mice at P56, but not at P28, displayed impaired performance in the test runs 24 hr after the training session, whereas no difference was found 1 hr after the training session (Figures S5D and S5E). Acute administration of clozapine improved their performance in NORT (Figure S5F). To address a function more specific to the cortex, mice were assessed by a T maze test at P56. DISC1 KD mice showed significantly fewer correct choices than did control mice, with delay intervals of 15 s, although there was no difference in required training time between the two groups (Figure S5G). In contrast, no difference was observed between DISC1 KD and control mice in the forced-swim test, a paradigm associated with depression (Figure S5H).

Next, in order to examine dopamine-associated behavioral deficits in DISC1 KD mice further, we challenged DISC1 KD mice with the psychostimulant methamphetamine. Although DISC1 KD mice did not differ from controls in spontaneous locomotion in the open field (Figure S6), DISC1 KD mice at P56, but not at P28, displayed hypersensitivity to administration of methamphetamine in locomotion (Figure 6A). Consistent with this result, we found that the increase of extracellular dopamine levels in nucleus accumbens in DISC1 KD mice was higher than that in controls after the administration of methamphetamine, although the basal levels of extracellular dopamine were slightly lower in DISC1 KD mice than in controls (Figure 6B).

DISCUSSION

There are two major conclusions in the present study. First, we report the potential to generate an animal model via in utero gene transfer in order to address an important question of how nonlethal deficits in early development may affect postnatal brain maturation of information processing and cognition in adulthood. Second, we show that transient knockdown of DISC1 in the pre- and perinatal stages, specifically in a lineage of pyramidal neurons mainly in PFC, leads to abnormalities in postnatal mesocortical dopaminergic maturation which results in overall disturbance in circuitry and several behavioral abnormalities in adulthood. Although there is precedence that insults in early development lead to delayed phenotypic manifestations in rodents (Koshibu et al., 2005; Lipska et al., 1993; Moore et al., 2006), the present study indicates the sequential link among pre-/perinatal disturbance in a specific genetic susceptibility factor (DISC1), the associated dendritic abnormalities in the neonatal stage, and, in turn, selective phenotypes in adolescence and adulthood.

This study may aid molecular understanding of how initial insults during early development disturb postnatal brain maturation for many years which results in full-blown onset of schizophrenia after puberty (Buka and Fan, 1999; Jaaro-Peled et al., 2009; McNeil, 1995). Although it is still being debated, brains from patients with schizophrenia show abnormalities in the cortex, especially in layers II/III, which include decreased arborization and smaller size of pyramidal neurons, as well as alteration

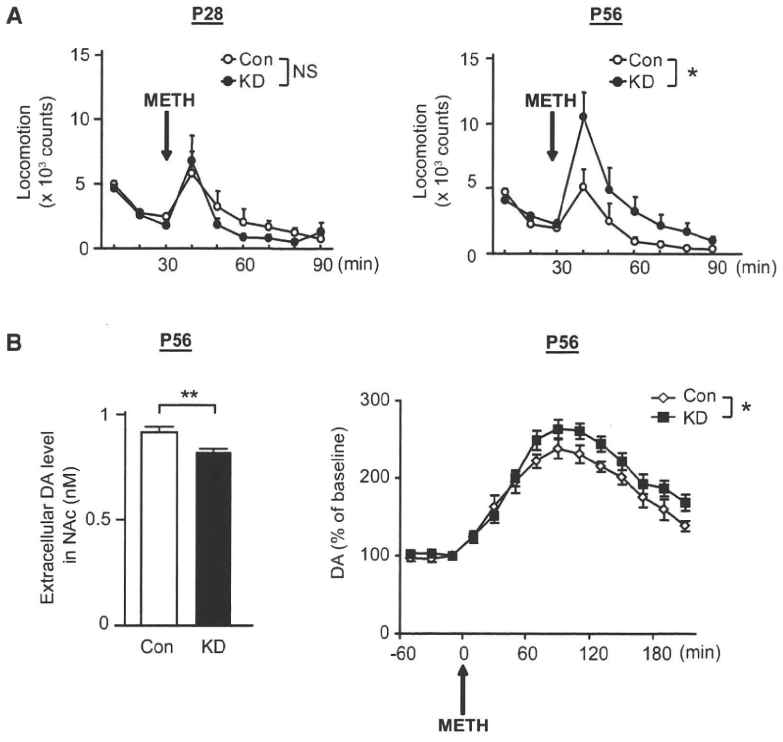

Figure 6. Hypersensitivity to the Psychostimulant Methamphetamine in DISC1 KD Mice after Puberty

(A) Methamphetamine (METH; 1 mg/kg, s.c.) -induced hyperactivity is augmented in DISC1 KD mice compared with Con mice, at P56 but not at P28 (*$p < 0.05$, $n = 6–10$ per condition).

(B) The extent of increase after METH challenge in levels of extracellular DA relative to those at the baseline is augmented in the nucleus accumbens (NAc) of DISC1 KD mice compared with Con mice at P56 (*$p < 0.05$, $n = 8$ per condition) (right), whereas mild but significant reduction of basal levels of extracellular DA is observed in KD mice (**$p < 0.01$, $n = 8$ per condition) (left).

Data are expressed as mean ± SEM.

in a subset of interneurons (Akbarian et al., 1995; Benes and Berretta, 2001; Glantz and Lewis, 2000; Guidotti et al., 2000; Lewis et al., 2005; Selemon and Goldman-Rakic, 1999). Furthermore, a decrease in tyrosine hydroxylase staining in schizophrenia patients has been reported, suggesting a reduction of dopaminergic innervation in the prefrontal cortex in schizophrenia (Akil et al., 1999). Primary defects for these cytoarchitectural changes may occur during neurodevelopment, because they are not accompanied by gliosis. Nevertheless, it has been unclear what kinds of neurodevelopmental defects result in such brain anatomical changes in patients with schizophrenia, with clinical onset 15–30 years after birth, characterized by psychosis and impaired cognition and information processing, and associated with aberrant neurotransmission, especially dopaminergic neurotransmission. The model in this study represents a majority of these objective characteristics reported in schizophrenia research. Therefore, to address the hierarchy and mechanistic links of these characteristics, this DISC1 model produced via in utero gene transfer may be useful. For example, an important question for future mechanistic studies with this model is how a decrease in tyrosine hydroxylase in all layers, or disturbance of postnatal maturation of mesocortical dopaminergic projections, is induced by dendritic abnormalities of the pyramidal neurons in layer II/III in the cortex in early development. Another question is how dysfunction of mesocortical dopaminergic projection affects its mesolimbic circuitry, including possible changes in dynamics of dopamine uptake and release, in the nucleus accumbens.

Although various types of genetically engineered animals, including inducible and conditional systems, have been developed, the in utero gene transfer technique with expression and/or shRNA constructs for RNAi may be a promising alternative methodology. We can select the target cell populations for genetic modulation specifically, by changing the direction of the electroporation (LoTurco et al., 2009). Thus, preferential targeting to a lineage of interneurons in the cortex or to hippocampal neurons is also technically feasible by targeting the electrodes toward ganglionic eminence or medial regions of the embryonic telencephalon, respectively (Borrell et al., 2005; Navarro-Quiroga et al., 2007). Furthermore, introduction of inducible expression constructs in in utero gene transfer will allow us to have better control of target gene expression (LoTurco et al., 2009; Manent et al., 2009; Matsuda and Cepko, 2007).

Many investigators have considered the possibility that adult brain function and behavior are influenced by neuronal network formation during development (Cannon et al., 2003; Harrison and Weinberger, 2005; Jaaro-Peled et al., 2009; Lisman et al., 2008), which is modulated by a combination of several genetic and environmental factors, and the concept of "pathway(s)" is more likely to mimic the mechanisms than the effect of a single gene product. By using the technical advantage of in utero transfer in which expression of more than one gene can be modified at one time by cotransfection of expression and/or RNAi constructs (Kamiya et al., 2008; Shu et al., 2004; Tsai et al., 2005; Young-Pearse et al., 2007), we will be able to test the synergistic influence or epistatic effect of multiple genetic factors. In a more general application, we propose that this method is useful in testing how modest but significant defects in neuronal network formation in early development lead to adult behavioral traits; furthermore, if potential variation between batches and animals is well controlled, this technique may also be utilized in trying to build novel animal models for various adult mental disorders, including schizophrenia, in which multiple risk factors play etiological roles during neurodevelopment.

EXPERIMENTAL PROCEDURES

Constructs

Short-hairpin RNA (shRNA) to DISC1 (5′-GGCAAACACTGTGAAGTGC-3′) was expressed by an H1 promoter-driven pSuper plasmid (Brummelkamp et al.,

2002). This shRNA was shown to effectively knock down DISC1 in cell cultures and in vivo via in utero gene transfer in previous publications from more than one research group (Kamiya et al., 2005, 2008; Mao et al., 2009). The duration of knockdown expression of genes by this H1-driven pSuper plasmid is dependent on the target molecules that we have tested so far (data not shown), and suppression of DISC1 was clearly transient in the developing cortex. Scrambled target sequence without homology to any known messenger RNA was used to produce the control RNAi. The expression construct used for rescue control experiments ($DISC1^R$) is described in Supplemental Information. The GFP expression construct is under the control of the CAG promoter.

In Utero Electroporation

In utero electroporation was performed by our published protocol with some modifications (Kamiya et al., 2005; Tabata and Nakajima, 2001). We used ICR mice, because neuropathological changes induced by the same shRNA to DISC1 had been characterized in this strain (Kamiya et al., 2005, 2008). Pregnant mice were anesthetized at E14 by intraperitoneal administration of 2,2,2-tribromoethanol in tert-amyl alcohol (0.4 mg/g). Two centimeter midline laparotomy was performed and the uterine horn was exposed. RNAi plasmids (2 μg/μl) together with GFP expression vector with CAG promoter (1 μg/μl) (molar ratio approximately 3:1) were injected into the bilateral ventricles with a glass micropipette made from a microcapillary tube (GD-1; Narishige). Injected plasmid solution contained Fast Green solution (0.001%) to monitor the injection. The embryo's head in the uterus was held between the tweezers-type electrode consisting of two disc electrodes of 5 mm diameter (CUY650-5; Tokiwa Science). Depending on which hemisphere was injected, the electrodes were oriented at a rough 20° outward angle from the midline and a rough 30° angle downward from an imaginary line from the olfactory bulbs to the caudal side of the cortical hemisphere. Electrode pulses (35V; 50 ms) were charged five times at intervals of 950 ms with an electroporator (CUY21E; Tokiwa Science). The uterine horn was placed back into the abdominal cavity and the abdominal wall and skin were sutured. All experiments were performed in accordance with the institutional guidelines for animal experiments.

Histology and Quantitative Analyses

Histological procedures were performed as previously described (Kamiya et al., 2005) with minor modifications. Brains were fixed with 4% paraformaldehyde, and coronal sections, including mPFC, were obtained with a cryostat at 20 μm (CM 1850; Leica). For immunohistochemistry, the following primary antibodies were used: anti-DISC1 (1: 100) (Ozeki et al., 2003), anti-tyrosine hydroxylase (TH) (1:100; Millipore), anti-parvalbumin (PV) (1:100; Sigma-Aldrich), anti-CaMKII (1:200; Upstate Biotechnology), and anti-GABA (1:200; Sigma-Aldrich). Fluorescent secondary antibodies conjugated to Alexa 488 and Alexa 568 (Molecular Probes) as well as biotin-conjugated secondaries were used for chromogen detection. Nuclei were labeled with Neurotrace Nissl 530/615 (Molecular Probes), propidium iodide (Molecular Probes), or DAPI (Molecular Probes). TUNEL staining was carried out as published (Yu et al., 2003).

To evaluate which types of cells were targeted by in utero gene transfer, the number of double-labeled cells with GFP together with specific cell markers, such as CaMKII (for pyramidal neurons), GABA (for interneurons), and GFAP (for astrocytes), was counted in a region of interest defined as 100 μm wide × 50 μm high in layers II/III in mPFC. Two regions of interest were randomly selected from three mice (a total of six regions). Images were acquired with a confocal microscope (LSM510; Carl Zeiss). The ratio of the number of double-labeled cells to that of cells with each cell marker was measured.

In order to quantify the effect of RNAi on expression of DISC1, the immunofluorescent intensity of DISC1 signal in each GFP-positive cell was measured by using MetaMorph software version 7.1 (MDS Analytical Technologies) after images were acquired with a confocal microscope (LSM510). The acquisition parameters were kept the same for all images. The intensity of the signal from randomly selected 10 GFP-positive cells in layers II/III of mPFC was quantitatively assessed in three DISC1 KD and three Con mice (i.e., 30 cells from DISC1 KD and 30 cells from Con mice). The signal in a region of equal size without cells in the lateral ventricle was subtracted as background.

To quantify immunoreactivity of TH and PV, a region of interest was defined as 800 μm wide × 1300 μm high in mPFC in the coronal sections (anteroposterior [AP]: +1.98 to +1.54 mm; mediolateral (ML): ± 0.8 mm from Bregma; dorsoventral [DV]: −1.75 to −3.05 mm from the dura) according to the atlas of Franklin and Paxinos (2007). Three images were acquired with a light microscope (Axioskop2 plus; Carl Zeiss) for each brain (six brains per DISC1 KD and control mice). The acquisition parameters were kept the same for all images. The areas of TH- or PV-positive cells/mm^2 were measured by the imaging software WinRoof (Mitani) after subtraction of the threshold value. The threshold was automatically measured at a minimum level by this software in the first image from a control mouse sample at P28 and was kept constant across all images.

For the procedures of morphological analysis of dendrites, see Supplemental Experimental Procedures.

Microdialysis

Microdialysis was carried out as previously described (Niwa et al., 2007) with a minor modification. A guide cannula (AG-6; Eicom) was implanted into the mPFC (15° angle from AP: +1.7 mm; ML: −1.0 mm from Bregma; DV: −1.5 mm from the dura) or nucleus accumbens (AP: +1.7 mm; ML: −0.8 mm from Bregma; DV: −4.0 mm from the dura). Ringer's solution (147 mM NaCl, 4 mM KCl, and 2.3 mM $CaCl_2$) was continuously perfused (1.0 μl/min). The dialysates were collected every 10 min and analyzed by high-performance liquid chromatography (HPLC) (Eicom). The levels of dopamine were also analyzed after the intraperitoneal injection of clozapine (3 mg/kg) (Sigma-Aldrich) or subcutaneous injection of methamphetamine (METH) (1 mg/kg) (Dainippon Sumitomo).

High-Performance Liquid Chromatography

Brains were removed rapidly, and each brain region was dissected out on ice according to the atlas of Franklin and Paxinos (2007). The brain homogenates were centrifuged at 20,000 × *g* for 15 min at 4°C, and the supernatants were mixed with 1 M sodium acetate to adjust to pH 3.0 for analysis by HPLC and by electrochemical detector (Eicom). The contents of norepinephrine (NE), dopamine (DA), and 5-hydroxytryptamine (5-HT) were determined as previously described (Miyamoto et al., 2002).

Electrophysiology

Mice were perfused with ice-cold artificial cerebrospinal fluid (ACSF) containing 125 mM NaCl, 25 mM $NaHCO_3$, 10 mM glucose, 3.5 mM KCl, 1.25 mM NaH_2PO_4, 0.5 mM (for P14) or 0.1 mM (for adult stage) $CaCl_2$, and 3 mM $MgCl_2$ (pH 7.4); osmolarity 285–295 mOsm. Coronal slices of brains at 400 μm (AP: +1.7 to 2.1 mm from Bregma) were made on a Vibratome and incubated in ACSF solution (35°C) oxygenated with 95% O_2 and 5% CO_2 for 60–70 min. For the recording ACSF, $CaCl_2$ was increased to 2 mM and $MgCl_2$ was decreased to 1 mM. All experiments were conducted at 33°C–35°C.

At P14, whole-cell recordings were performed from the GFP-labeled pyramidal neurons in layers II/III in the mPFC. Patch pipettes (3–6 MΩ) were filled with 115 mM K gluconate, 20 mM KCl, 10 mM KOH, 2 mM $MgCl_2$, 4 mM Na_2ATP, 1 mM NaGTP, 10 mM HEPES, 0.4 mM EGTA (pH 7.2). The τ_m was obtained by single-exponential fitting and the membrane capacitance was calculated.

At adult stage, whole-cell recordings were performed from pyramidal neurons in layers V/VI in the mPFC, where GFP-labeled cells were located in layers II/III, and identified under visual guidance by using infrared differential interference contrast video microscopy. Electrical stimulation (1 pulse, 0.2–1.4 mA) was applied through an electrode consisting of tungsten wire. The stimulating electrode was placed near layer I, 0.7–1 mm lateral to the location of whole-cell recordings in layers V/VI . Patch pipettes (9–12 MΩ) were filled with 115 mM K gluconate, 10 mM HEPES, 2 mM $MgCl_2$, 20 mM KCl, 2 mM MgATP, 2 mM Na_2ATP, and 0.3 mM GTP (pH 7.3); 285–295 mOsm. All bath-applied drugs, such as quinpirole and CNQX, were applied in the recording solution at known concentrations. Single pulses of current were delivered every 20 s, and stimulation current was adjusted so as to produce 4–10 mV postsynaptic potentials with reliable amplitude. Baseline responses to stimulation were recorded prior to adding quinpirole (5 μM) for 5–6 min. The magnitude of evoked responses was averaged over the baseline and compared to

the average during the 5 min time interval from +2 to +7 min after quinpirole addition. This period was chosen for consistency, with differences revealed by previous investigations of D2 modulation of PFC activity in rodent models of schizophrenia (Tseng et al., 2008).

Behavioral Analysis

Prepulse Inhibition

Prepulse inhibition (Arguello and Gogos, 2006) of the acoustic startle response was measured using an SR-LAB System (San Diego Instruments). The stimulus onset consisted of a 20 ms prepulse, a 100 ms delay, and then a 40 ms startle pulse. The intensity of the prepulse was 8 or 16 dB above the 70 dB background noise. The amount of prepulse inhibition was calculated as a percentage of the 120 dB acoustic startle response: 100 – [(startle reactivity on prepulse + startle pulse)/startle reactivity on startle pulse] × 100. PPI tests were also performed 30 min after the intraperitoneal injection of clozapine (3 mg/kg).

Locomotor Activity

To measure spontaneous activity, mice were placed in a transparent acrylic cage, and locomotion and rearing were measured every 5 min for 60 min by using digital counters with infrared sensors (Scanet SV-10; Merquest) as described previously (Miyamoto et al., 2002). To measure methamphetamine (METH) -induced hyperactivity, mice received one subcutaneous injection of METH (1 mg/kg) after 30 min of prehabituation in a cage (Miyamoto et al., 2004).

Unbiased Assessment in Experimental Procedures

To avoid experimental bias by investigators, in utero surgery and all analyses, including those for DISC1 immunostaining and behavioral tests, were conducted by multiple investigators in a systematic manner as follows: an investigator conducted in utero surgery without knowing the identification of constructs. Furthermore, investigators conducted several assays without knowing the identification of mice (either DISC1 KD or controls).

Statistical Analysis

The Student's *t* test was used in comparing two sets of data. Statistical differences among more than three groups were determined using one-way analysis of variance (ANOVA), two-way ANOVA, or ANOVA with repeated measures followed by Bonferroni multiple comparison tests. A value of $p < 0.05$ was considered statistically significant. All data are expressed as mean ± SEM.

SUPPLEMENTAL INFORMATION

Supplemental Information includes six figures and Supplemental Experimental Procedures and can be found with this article online at doi:10.1016/j.neuron.2010.01.019.

ACKNOWLEDGMENTS

We thank Dr. Pamela Talalay and Dr. Eva Anton for critical reading and Ms. Yukiko Lema for organizing the manuscript. This work was supported by U.S. Public Heath Service grant MH-069853 (A.S.), Silvio O. Conte Center grants MH-084018 (A.S.) and MH-088753 (A.S.), and foundation grants from Stanley (A.S.), S-R (A.S., A.K.), RUSK (A.S.), and NARSAD (A.S., A.K., H.J.-P.). This work was also supported by grants from JSPS (T.N., K.N., M.N.), MEXT (T.N., K.N.), MARC (T.N.), MHLW (T.N., K.K.), Sumitomo (K.N.), Naito (K.N.), Academic Frontier Project (T.N.), and Takeda (T.N., K.N.).

Accepted: January 14, 2010
Published: February 24, 2010

REFERENCES

Akbarian, S., Kim, J.J., Potkin, S.G., Hagman, J.O., Tafazzoli, A., Bunney, W.E., Jr., and Jones, E.G. (1995). Gene expression for glutamic acid decarboxylase is reduced without loss of neurons in prefrontal cortex of schizophrenics. Arch. Gen. Psychiatry *52*, 258–266.

Akil, M., Pierri, J.N., Whitehead, R.E., Edgar, C.L., Mohila, C., Sampson, A.R., and Lewis, D.A. (1999). Lamina-specific alterations in the dopamine innervation of the prefrontal cortex in schizophrenic subjects. Am. J. Psychiatry *156*, 1580–1589.

Anderson, S.A., Eisenstat, D.D., Shi, L., and Rubenstein, J.L. (1997). Interneuron migration from basal forebrain to neocortex: dependence on Dlx genes. Science *278*, 474–476.

Arguello, P.A., and Gogos, J.A. (2006). Modeling madness in mice: one piece at a time. Neuron *52*, 179–196.

Benes, F.M., and Berretta, S. (2001). GABAergic interneurons: implications for understanding schizophrenia and bipolar disorder. Neuropsychopharmacology *25*, 1–27.

Benes, F.M., Taylor, J.B., and Cunningham, M.C. (2000). Convergence and plasticity of monoaminergic systems in the medial prefrontal cortex during the postnatal period: implications for the development of psychopathology. Cereb. Cortex *10*, 1014–1027.

Borrell, V., Yoshimura, Y., and Callaway, E.M. (2005). Targeted gene delivery to telencephalic inhibitory neurons by directional in utero electroporation. J. Neurosci. Methods *143*, 151–158.

Brummelkamp, T.R., Bernards, R., and Agami, R. (2002). A system for stable expression of short interfering RNAs in mammalian cells. Science *296*, 550–553.

Buka, S.L., and Fan, A.P. (1999). Association of prenatal and perinatal complications with subsequent bipolar disorder and schizophrenia. Schizophr. Res. *39*, 113–119.

Cannon, T.D., van Erp, T.G., Bearden, C.E., Loewy, R., Thompson, P., Toga, A.W., Huttunen, M.O., Keshavan, M.S., Seidman, L.J., and Tsuang, M.T. (2003). Early and late neurodevelopmental influences in the prodrome to schizophrenia: contributions of genes, environment, and their interactions. Schizophr. Bull. *29*, 653–669.

Chen, J., Lipska, B.K., and Weinberger, D.R. (2006). Genetic mouse models of schizophrenia: from hypothesis-based to susceptibility gene-based models. Biol. Psychiatry *59*, 1180–1188.

Franklin, B.J.K., and Paxinos, G. (2007). The Mouse Brain in Stereotaxic Coordinates (San Diego: Academic Press).

Glantz, L.A., and Lewis, D.A. (2000). Decreased dendritic spine density on prefrontal cortical pyramidal neurons in schizophrenia. Arch. Gen. Psychiatry *57*, 65–73.

Goto, Y., and Grace, A.A. (2007). The dopamine system and the pathophysiology of schizophrenia: a basic science perspective. Int. Rev. Neurobiol. *78C*, 41–68.

Guidotti, A., Auta, J., Davis, J.M., Di-Giorgi-Gerevini, V., Dwivedi, Y., Grayson, D.R., Impagnatiello, F., Pandey, G., Pesold, C., Sharma, R., et al. (2000). Decrease in reelin and glutamic acid decarboxylase67 (GAD67) expression in schizophrenia and bipolar disorder: a postmortem brain study. Arch. Gen. Psychiatry *57*, 1061–1069.

Harrison, P.J., and Weinberger, D.R. (2005). Schizophrenia genes, gene expression, and neuropathology: on the matter of their convergence. Mol. Psychiatry *10*, 40–68.

Jaaro-Peled, H., Hayashi-Takagi, A., Seshadri, S., Kamiya, A., Brandon, N.J., and Sawa, A. (2009). Neurodevelopmental mechanisms of schizophrenia: understanding disturbed postnatal brain maturation through neuregulin-1-ErbB4 and DISC1. Trends Neurosci. *32*, 485–495.

Kamiya, A., Kubo, K., Tomoda, T., Takaki, M., Youn, R., Ozeki, Y., Sawamura, N., Park, U., Kudo, C., Okawa, M., et al. (2005). A schizophrenia-associated mutation of DISC1 perturbs cerebral cortex development. Nat. Cell Biol. *7*, 1167–1178.

Kamiya, A., Tan, P.L., Kubo, K., Engelhard, C., Ishizuka, K., Kubo, A., Tsukita, S., Pulver, A.E., Nakajima, K., Cascella, N.G., et al. (2008). Recruitment of PCM1 to the centrosome by the cooperative action of DISC1 and BBS4: a candidate for psychiatric illnesses. Arch. Gen. Psychiatry *65*, 996–1006.